Acta Mechanica

Nonlocal frequency analysis of nanosensors with different boundary conditions and attached distributed biomolecules: an approximate method

--Manuscript Draft--

Manuscript Number:	ACME-D-15-00543R4
Full Title:	Nonlocal frequency analysis of nanosensors with different boundary conditions and attached distributed biomolecules: an approximate method
Article Type:	Original Paper
Keywords:	Nonlocal elasticity, Frequency analysis, Nanosensors, biomolecules, boundary conditions
Corresponding Author:	Maria Anna De Rosa School of Engineering-University of Basilicata ITALY
Corresponding Author Secondary Information:	
Corresponding Author's Institution:	School of Engineering-University of Basilicata
Corresponding Author's Secondary Institution:	
First Author:	Maria Anna De Rosa
First Author Secondary Information:	
Order of Authors:	Maria Anna De Rosa
	Maria Lippiello, PhD
	Hector D Martin, PhD student
	Marcelo T Piovan, Professor
Order of Authors Secondary Information:	
Funding Information:	
Abstract:	Nanosensors are simple engineering devices designed to detect and convey informations about nanoparticles and biomolecules. The nanosized mass sensors are based on the fact that the resonant frequency is sensitive to the resonator and the attached mass. The change of the attached mass on the resonator causes the resonant frequency to deviate from its original value. The key challenge in mass detection is in quantifying the changes in the resonant frequencies due to the added masses. The present paper deals with the free vibration analysis of single-walled carbon nanotube with attached distributed mass, located in a generic position. According to the nonlocal Euler-Bernoulli beam theory a system of three equations of motion, of a single-walled carbon nanotube with a added mass, is derived. Using an approximate method, generalized nondimensional calibration constants are derived for an explicit relationship between the added mass, the nonlocal parameter and the frequency shift. Numerical results for different boundary conditions, nonlocal coefficient are performed in order to evaluate the effect of the added mass.

Dear Editor,

following your suggestions, the Authors have corrected the minor error in A11-A13.

Many regards

Maria Anna De Rosa

Nonlocal frequency analysis of nanosensors with different boundary conditions and attached distributed biomolecules: an approximate method

M.A. De Rosa[a,*], M. Lippiello[b], H.D. Martin[c], M.T. Piovan[d]

[a] *School of Engineering, University of Basilicata, Viale dell'Ateneo Lucano 10, 85100 Potenza, Italy*

[b] *Department of Structures for Engineering and Architecture, University of Naples "Federico II", Via Forno Vecchio 36, 80134 Napoli, Italy*

[c] *Facultad Regional Reconquista UTN. Parque Industrial Reconquista, (3560) Reconquista, Santa Fe, Argentina*

[d] *Centro de investigaciones de Mecanica Teorica y Aplicada, Universidad Tecnologica Nacional FRBB., 11 de Abril 461, B8000LMI, Bahia Blanca, Argentina*

Abstract

Nanosensors are simple engineering devices designed to detect and convey informations about nanoparticles and biomolecules. The nanosized mass sensors are based on the fact that the resonant frequency is sensitive to the resonator and the attached mass. The change of the attached mass on the resonator causes the resonant frequency to deviate from its original value. The key challenge in mass detection is in quantifying the changes in the resonant frequencies due to the added masses.

The present paper deals with the free vibration analysis of single-walled carbon nanotube with attached distributed mass, located in a generic position. According to the nonlocal Euler-Bernoulli beam theory a system of three equations of motion, of a single-walled carbon nanotube with a added mass, is derived. Using an approximate method, generalized nondimensional calibration constants are derived for an explicit relationship between the added mass, the nonlocal parameter and the frequency shift. Numerical results for different boundary conditions, nonlocal coefficient are performed in

*Corresponding author

Email addresses: maria.derosa@unibas.it (M.A. De Rosa), maria.lippiello@unina.it (M. Lippiello), hmartin@frrq.utn.edu.ar (H.D. Martin), mpiovan@frbb.utn.edu.ar (M.T. Piovan)

order to evaluate the effect of the added mass.

Keywords: Nonlocal elasticity, Frequency analysis, Nanosensors, biomolecules, boundary conditions

1. Introduction

Carbon nanotubes (CNTs) constitute a prominent example of nanomaterials and nanostructures which have stimulated several studies in nanotechnology applications and nano-scale engineering materials. Their discovery, since the publication of Iijima's paper [1] in 1991, led to an explosion of interest within the scientific community and has inspired intensive studies in a variety of fields of engineering due to their excellent physical properties, as revealed from both theoretical and experimental studies available in the literature, ([2]-[5]). These remarkable properties of carbon nanotubes have been investigated for devices such as scanning probes, nanoelectronic devices, nanoscale sensors, biomedical devices, and others. As a result, progressive research activities regarding CNTs have been ongoing in recent years and there is a wide range of applications, as nanooscillators, nanoelectronics, nanocomposites and nanosensors, in which the vibrational characteristics of CNTs are significant. Moreover, such features make CNTs promising candidates for resolution mass sensor and several studies have investigated the use of CNTs as a mass sensor, (see for example ([6]-[16]).

From a theoretical point of view, the nano-scale of these structures suggests an atomistic model, but this approach turns out to be very expensive, so that continuum mechanical models have been effectively used to study mechanical behaviors of CNTs. For example, the classical Euler-Bernoulli beam theory was employed to model a nanomechanical resonator, ([10],[17]). Although the classical continuum theory is able to predict the behaviors of nanostructures, it is found to be inadequate because of ignoring the small size effects. Recently, nonlocal elastic continuum models have been used for studying the mechanical behaviour of CNTs including beam models. Their application to the analysis of CNTs allows to evaluate the small-scale effects influence. The origins of the nonlocal theory of elasticity go to pioneering works, published in early 80s, by Eringen [18]. The theory of nonlocal elasticity finds general application in the area of nanostructural study such as in nanorods, nanobeams, nanoplates, nanorings, carbon nanotubes, graphenes,

nanoswitches and protein microtubules. Via nonlocal elasticity theory the small-scale effects are incorporated by assuming that the stress, at a given reference point, is considered to be a function of the strain field at all points of the body. A good review on nonlocal elasticity is presented in [19]: Reddy reports a complete development of the classical and shear deformation beam theories using the nonlocal constitutive differential equations and derives the solutions for bending, buckling and natural frequencies problems. In recent years, many researchers have applied the nonlocal elasticity concept to bending, buckling and vibration analysis of nanostructures. Although initiated by the work of Eringen, the possibility of using the nonlocal continuum theory in the field of nanotechnology was first reported by Peddieson et al. [20]. These Authors have used nonlocal Euler-Bernoulli model for static analysis of nano-beams and particular attention has been paid to cantilever beams which are often used as actuators in small scale-systems. Further applications of the nonlocal elasticity theory have been employed in studying the buckling ([21],[22]) and vibration problems, by applying Euler- Bernoulli beam and shell theories and Timoshenko beam theory, in CNTs ([21]-[25]). Following these ideas, Lee et al. in [26] used the nonlocal Euler-Bernoulli beam theory to analyze the frequency shift of carbon nanotube with an attached mass based upon mass-sensors. In addition, the Authors have analyzed the effects of nonlocal parameter, attached mass and its location on the frequency shift value. Aydogdu and Filiz [27] have studied axial vibration behaviour of single-walled carbon nanotube based mass sensors and have analyzed the effects of CNT length, attached mass, position and nonlocal parameters on vibration of SWCNTs. Shen et al. [28] have investigated the transverse vibration of the CNT-based micro-mass sensor based on the nonlocal Timoshenko beam theory.

Nanosensors are simple engineering devices designed to detect and convey informations about nanoparticles and biomolecules. The nanosized mass sensors are based on the fact that the resonant frequency is sensitive to the resonator and the attached mass. The change of the attached mass on the resonator causes the resonant frequency to deviate from its original value. The key challenge in mass detection is the quantifycation of variations in the resonant frequencies due to the added masses. Recently, mass detection based on the resonating nanomechanical tools has been subject of growing interests as for example in ([29]-[32]).

The present note deals with the approximate problem of the single-walled carbon nanotube with an attached distributed mass, located in a generic po-

sition, in the presence of nonlocal effect and under different boundary conditions. Applying the nonlocal Euler- Bernoulli beam theory a system of three equations of motion is derived. Using an approximate method, generalized nondimensional calibration constants are derived for an explicit relationship between the added mass, the nonlocal parameter and the frequency shift. For this purpose, integral expressions of calibration parameters are given and their values are used to derive the fundamental natural frequency, which is obtained by employing an extension of classical Rayleigh quotient to the case of non-local Euler-Bernoulli beams and in presence of a distributed mass. The frequency shift is defined as the difference between the fundamental frequencies of single-walled carbon nanotube with and without the attached distributed mass, and it is usefully in order to assess qualitatively the vibrational behaviour of the nanosensor. Once the relative frequency shift is calculated, it is possible to determine the non dimensional mass expression. Furthermore, because of the calibration constants change depending on the boundary conditions, in the present paper the fundamental natural frequency expression for clamped-free, clamped-clamped, simply-supported, clamped-supported and clamped-sliding nanosensors is derived. From the literature it has been found that nonlocal elasticity has been used only in two cases: clamped-free and clamped -clamped nanotube nanotubes with the attached mass. Finally, numerical results are illustrated and compared with some results of literature.

2. Formulation of the problem

A typical single-walled carbon nanotube (SWCNT) with an added distributed mass m, located between γ_1L and γ_2L, is shown in Figure 1. The single-walled carbon nanotube with span L has cross sectional area A, second moment of area I, Young modulus E and mass density ρ.

According to Hamilton Principle it is possible to write:

$$\int_{t_1}^{t_2} (\delta \, \mathrm{T}(t) - \delta E(t)) \, \mathrm{dt} = 0 \tag{1}$$

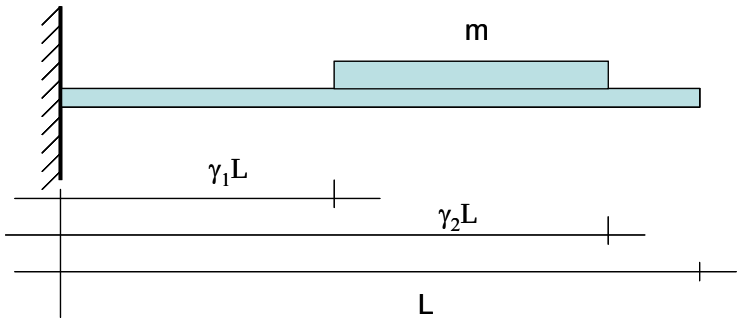

Figure 1: Geometrical properties of the nanotube

where

$$T = \frac{1}{2}\int_0^{\gamma_1 L} \rho A \left(\frac{\partial v_1(z,t)}{\partial t}\right)^2 \mathrm{dz} + \frac{1}{2}\int_{\gamma_1 L}^{\gamma_2 L} \rho A \left(\frac{\partial v_2(z,t)}{\partial t}\right)^2 \mathrm{dz} + \frac{1}{2}\int_{\gamma_2 L}^{L} \rho A \left(\frac{\partial v_3(z,t)}{\partial t}\right)^2 \mathrm{dz} + \frac{1}{2}\int_{\gamma_1 L}^{\gamma_2 L} M \left(\frac{\partial v_2(z,t)}{\partial t}\right)^2 \mathrm{dz} \qquad (2)$$

is the kinetic energy of the structure. It is given by the sum of the kinetic energies of the three sections, and of the kinetic energy of the additional mass. The three displacements functions v_1, v_2 and v_3 vary between $(0, \gamma_1 L)$, $(\gamma_1 L, \gamma_2 L)$, and $(\gamma_2 L, L)$, respectively. The total potential energy can be

expressed as:

$$E = L - P = \frac{1}{2}\int_0^{\gamma_1 L} \mathrm{EI}\left(\frac{\partial^2 v_1(z,t)}{\partial z^2}\right)^2 \mathrm{dz} + \frac{1}{2}\int_{\gamma_1 L}^{\gamma_2 L} \mathrm{EI}\left(\frac{\partial^2 v_2(z,t)}{\partial z^2}\right)^2 \mathrm{dz} + \frac{1}{2}\int_{\gamma_2 L}^{L} \mathrm{EI}\left(\frac{\partial^2 v_3(z,t)}{\partial z^2}\right)^2 \mathrm{dz} - \int_0^{\gamma_1 L} \rho A \frac{\partial^2 v_1(z,t)}{\partial t^2} \left(e_0 a\right)^2 \frac{\partial^2 v_1(z,t)}{\partial z^2} \mathrm{dz} - \int_{\gamma_1 L}^{\gamma_2 L} \rho A \frac{\partial^2 v_2(z,t)}{\partial t^2} \left(e_0 a\right)^2 \frac{\partial^2 v_2(z,t)}{\partial z^2} \mathrm{dz} - \int_{\gamma_2 L}^{L} \rho A \frac{\partial^2 v_3(z,t)}{\partial t^2} \left(e_0 a\right)^2 \frac{\partial^2 v_3(z,t)}{\partial z^2} \mathrm{dz} \tag{3}$$

where L is the sum of the strain energy of the nanotube and P is the potential energy of the inertial force $\left(\rho A \frac{\partial^2 v(z,t)}{\partial t^2}\right)$ due to the additional displacement $\left(e_0 a\right)^2 \frac{\partial^2 v(z,t)}{\partial z^2}$, as explained at length in [32]. In this paper the Hamilton principle has been employed in order to obtain the correct equations together with the boundary conditions, so confirming the direct approach of Reddy-Pang [33], where the nonlocal Eringen theory has been used. On the other hand, Challamel at al. [34], have shown how the Eringen model can be derived from a variational approach, where some nonconservative terms must be included. Nevertheless, their boundary conditions turn out to be coincident with ours, even for the cantilever beam. In Eq. (3), e_0 is a constant which has to be experimentally determined for each material, a is an internal characteristic length.

The first variation of these two energies can be easily calculated as, so that (1) gives:

$$\int_{t_1}^{t_2}\Big(\int_0^{\gamma_1 L}\rho A\frac{\partial v_1(z,t)}{\partial t}\delta\frac{\partial v_1(z,t)}{\partial t}\,\mathrm{dz}+\int_{\gamma_1 L}^{\gamma_2 L}\rho A\frac{\partial v_2(z,t)}{\partial t}\delta\frac{\partial v_2(z,t)}{\partial t}\,\mathrm{dz}+$$
$$\int_{\gamma_2 L}^{L}\rho A\frac{\partial v_3(z,t)}{\partial t}\delta\frac{\partial v_3(z,t)}{\partial t}\,\mathrm{dz}+\frac{1}{2}\int_{\gamma_1 L}^{\gamma_2 L}M\frac{\partial v_2(z,t)}{\partial t}\delta\frac{\partial v_2(z,t)}{\partial t}\,\mathrm{dz}-$$
$$\int_0^{\gamma_1 L}\left(EI\frac{\partial^2 v_1(z,t)}{\partial z^2}\delta\frac{\partial^2 v_1(z,t)}{\partial z^2}-(e_0a)^2\rho A\frac{\partial^2 v_1(z,t)}{\partial t^2}\delta\frac{\partial^2 v_1(z,t)}{\partial z^2}\right)\mathrm{dz}-$$
$$\int_{\gamma_1 L}^{\gamma_2 L}\left(EI\frac{\partial^2 v_2(z,t)}{\partial z^2}\delta\frac{\partial^2 v_2(z,t)}{\partial z^2}-(e_0a)^2\rho A\frac{\partial^2 v_2(z,t)}{\partial t^2}\delta\frac{\partial^2 v_2(z,t)}{\partial z^2}\right)\mathrm{dz}-$$
$$\int_{\gamma_2 L}^{L}\left(EI\frac{\partial^2 v_3(z,t)}{\partial z^2}\delta\frac{\partial^2 v_3(z,t)}{\partial z^2}-(e_0a)^2\rho A\frac{\partial^2 v_3(z,t)}{\partial t^2}\delta\frac{\partial^2 v_3(z,t)}{\partial z^2}\right)\mathrm{dz}\Big)\mathrm{dt}=0 \tag{4}$$

All the terms in (4), as already reported in [35], should be integrated by parts (see Appendix A).

The equations of motion of free-vibration of a nanotube, in the presence of the nonlocal effect and added mass, are:

$$\begin{aligned}
&\mathrm{EI}\,\frac{\partial^4 v_1(z,t)}{\partial z^4}-(e_0a)^2\,\rho\mathrm{A}\frac{\partial^4 v_1(z,t)}{\partial z^2\partial t^2}+\rho\mathrm{A}\frac{\partial^2 v_1(z,t)}{\partial t^2}=0, \qquad 0<z<\gamma_1 L\\
&\mathrm{EI}\,\frac{\partial^4 v_2(z,t)}{\partial z^4}-(e_0a)^2\,\rho\mathrm{A}\frac{\partial^4 v_2(z,t)}{\partial z^2\partial t^2}+(\rho\mathrm{A}+\mathrm{m})\frac{\partial^2 v_2(z,t)}{\partial t^2}=0,\ \gamma_1 L<z<\gamma_2 L\\
&\mathrm{EI}\,\frac{\partial^4 v_3(z,t)}{\partial z^4}-(e_0a)^2\,\rho\mathrm{A}\frac{\partial^4 v_3(z,t)}{\partial z^2\partial t^2}+\rho\mathrm{A}\frac{\partial^2 v_3(z,t)}{\partial t^2}=0, \quad \gamma_2 L<z<L
\end{aligned} \tag{5}$$

and the corresponding general boundary conditions of the equations system (5) are reported in Appendix A.

Assuming the following harmonic solution

$$v_j(z,t)=v_j(z)e^{i\omega t},\quad j=1,2,3 \tag{6}$$

where ω is the angular frequency and i is the conventional imaginary number $i=\sqrt{-1}$, the system of three equations of motion (5) becomes:

$$
\begin{aligned}
&\mathrm{EI}\,\frac{\partial^4 v_1(z)}{\partial z^4} + \omega^2 \left(e_0 a\right)^2 \rho\mathrm{A}\frac{\partial^4 v_1(z)}{\partial z^2} - \omega^2 \rho\mathrm{A} v_1(z) = 0, \qquad 0 < z < \gamma_1 L \\
&\mathrm{EI}\,\frac{\partial^4 v_2(z)}{\partial z^4} + \omega^2 \left(e_0 a\right)^2 \rho\mathrm{A}\frac{\partial^4 v_2(z)}{\partial z^2} - \omega^2 (\rho\mathrm{A} + \mathrm{m}) v_2(z) = 0, \ \gamma_1 L < z < \gamma_2 L \\
&\mathrm{EI}\,\frac{\partial^4 v_3(z)}{\partial z^4} + \omega^2 \left(e_0 a\right)^2 \rho\mathrm{A}\frac{\partial^4 v_3(z)}{\partial z^2} - \omega^2 \rho\mathrm{A} v_3(z) = 0. \qquad \gamma_2 L < z < L
\end{aligned}
\tag{7}
$$

Starting from the equations of motion (7), it is now possible to multiply each term by a trial function $y(z)$ and to integrate each of them in their domain, as follows

$$
\begin{aligned}
&\int_0^{\gamma_1 L} \mathrm{EI}\,\frac{\partial^4 v_1(z)}{\partial z^4} y(z)\mathrm{dz} + \\
&\int_0^{\gamma_1 L} \omega^2 \left(e_0 a\right)^2 \rho\mathrm{A}\frac{\partial^2 v_1(z)}{\partial z^2} y(z)\mathrm{dz} - \int_0^{\gamma_1 L} \omega^2 \rho\mathrm{A} v_1(z) y(z)\mathrm{dz} = 0, \qquad 0 < z < \gamma_1 L \\
&\int_{\gamma_1 L}^{\gamma_2 L} \mathrm{EI}\,\frac{\partial^4 v_2(z)}{\partial z^4} y(z)\mathrm{dz} + \\
&\int_{\gamma_1 L}^{\gamma_2 L} \omega^2 \left(e_0 a\right)^2 \rho\mathrm{A}\frac{\partial^2 v_2(z)}{\partial z^2} y(z)\mathrm{dz} - \int_{\gamma_1 L}^{\gamma_2 L} \omega^2 (\rho\mathrm{A} + \mathrm{m}) v_2(z) y(z)\mathrm{dz} = 0, \qquad \gamma_1 L < z < \gamma_2 L \\
&\int_{\gamma_2 L}^{L} \mathrm{EI}\,\frac{\partial^4 v_3(z)}{\partial z^4} y(z)\mathrm{dz} + \\
&\int_{\gamma_2 L}^{L} \omega^2 \left(e_0 a\right)^2 \rho\mathrm{A}\frac{\partial^2 v_3(z)}{\partial z^2} y(z)\mathrm{dz} - \int_{\gamma_2 L}^{L} \omega^2 \rho\mathrm{A} v_3(z) y(z)\mathrm{dz} = 0, \qquad \gamma_2 L < z < L
\end{aligned}
\tag{8}
$$

and the resulting integrals can be summed up

$$
\begin{aligned}
&\int_0^{\gamma_1 L} \mathrm{EI}\,\frac{\partial^4 v_1(z)}{\partial z^4} y(z)\mathrm{dz} + \int_0^{\gamma_1 L} \omega^2 \left(e_0 a\right)^2 \rho\mathrm{A}\frac{\partial^2 v_1(z)}{\partial z^2} y(z)\mathrm{dz} - \int_0^{\gamma_1 L} \omega^2 \rho\mathrm{A} v_1(z) y(z)\mathrm{dz} + \\
&\int_{\gamma_1 L}^{\gamma_2 L} \mathrm{EI}\,\frac{\partial^4 v_2(z)}{\partial z^4} y(z)\mathrm{dz} + \int_{\gamma_1 L}^{\gamma_2 L} \omega^2 \left(e_0 a\right)^2 \rho\mathrm{A}\frac{\partial^2 v_2(z)}{\partial z^2} y(z)\mathrm{dz} - \int_{\gamma_1 L}^{\gamma_2 L} \omega^2 (\rho\mathrm{A} + \mathrm{m}) v_2(z) y(z)\mathrm{dz} + \\
&\int_{\gamma_2 L}^{L} \mathrm{EI}\,\frac{\partial^4 v_3(z)}{\partial z^4} y(z)\mathrm{dz} + \int_{\gamma_2 L}^{L} \omega^2 \left(e_0 a\right)^2 \rho\mathrm{A}\frac{\partial^2 v_3(z)}{\partial z^2} y(z)\mathrm{dz} - \int_{\gamma_2 L}^{L} \omega^2 \rho\mathrm{A} v_3(z) y(z)\mathrm{dz} = 0.
\end{aligned}
\tag{9}
$$

Because of the additive properties of the integrals, it is possible to reduce to integrals between 0 and L:

$$\int_0^L \mathrm{EI}\,\frac{\partial^4 v(z)}{\partial z^4} y(z)\mathrm{dz} + \omega^2 \int_0^L (e_0 a)^2\,\rho\mathrm{A}\frac{\partial^2 v(z)}{\partial z^2} y(z)\mathrm{dz} - \omega^2 \int_0^L \rho\mathrm{A} v(z) y(z)\mathrm{dz} - \omega^2 \int_{\gamma_1 L}^{\gamma_2 L} \mathrm{m} v(z) y(z)\mathrm{dz} = 0. \tag{10}$$

where $v(z)$ denotes the displacement function along the whole span. Two successive integrations by parts can be performed (see Appendix B), so that equation (10) becomes:

$$\int_0^L \mathrm{EI}\,\frac{\partial^2 v(z)}{\partial z^2}\frac{\partial^2 y(z)}{\partial z^2}\mathrm{dz} - \omega^2 \int_0^L \rho\mathrm{A} v(z) y(z)\mathrm{dz} - \omega^2 \int_{\gamma_1 L}^{\gamma_2 L} \mathrm{m} v(z) y(z)\mathrm{dz} + \int_0^L \omega^2\,(e_0 a)^2\,\rho\mathrm{A} v(z)\frac{\partial^2 y(z)}{\partial z^2}\mathrm{dz} + \left[\mathrm{EI}\frac{\partial^3 v(z)}{\partial z^3} y(z)\right]_0^L - \left[\mathrm{EI}\,\frac{\partial^2 v(z)}{\partial z^2}\frac{\partial y(z)}{\partial z}\right]_0^L + \left[\omega^2\,(e_0 a)^2\,\rho\mathrm{A}\frac{\partial v(z)}{\partial z} y(z)\right]_0^L - \left[\omega^2\,(e_0 a)^2\,\rho\mathrm{A} v(z)\frac{\partial y(z)}{\partial z}\right]_0^L = 0. \tag{11}$$

Finally, the integral terms and the finite terms should be zero separately:

$$\int_0^L \mathrm{EI}\,\frac{\partial^2 v(z)}{\partial z^2}\frac{\partial^2 y(z)}{\partial z^2}\mathrm{dz} - \omega^2 \int_0^L \rho\mathrm{A} v(z) y(z)\mathrm{dz} - \omega^2 \int_{\gamma_1 L}^{\gamma_2 L} \mathrm{m} v(z) y(z)\mathrm{dz} + \int_0^L \omega^2\,(e_0 a)^2\,\rho\mathrm{A} v(z)\frac{\partial^2 y(z)}{\partial z^2}\mathrm{dz} = 0, \tag{12}$$

$$\left[\mathrm{EI}\,\frac{\partial^3 v(z)}{\partial z^3} y(z)\right]_0^L - \left[\mathrm{EI}\frac{\partial^2 v(z)}{\partial z^2}\frac{\partial y(z)}{\partial z}\right]_0^L + \left[\omega^2\,(e_0 a)^2\,\rho\mathrm{A}\frac{\partial v(z)}{\partial z} y(z)\right]_0^L - \left[\omega^2\,(e_0 a)^2\,\rho\mathrm{A} v(z)\frac{\partial y(z)}{\partial z}\right]_0^L = 0. \tag{13}$$

If the nondimensional abscissa $\zeta = \frac{z}{L}$ is introduced in equations (12-13), the equation of motion (12) becomes:

$$\frac{\mathrm{EI}}{L^3}\int_0^1 \frac{\partial^2 v(\zeta)}{\partial\zeta^2}\frac{\partial^2 y(\zeta)}{\partial\zeta^2}\mathrm{d}\zeta + \frac{\omega^2\left(e_0 a\right)^2 \rho \mathrm{A} L}{L^2}\int_0^1 v(\zeta)\frac{\partial^2 y(\zeta)}{\partial\zeta^2}\mathrm{d}\zeta -$$
$$\omega^2 \rho \mathrm{A} L\int_0^1 v(\zeta)y(\zeta)\mathrm{d}\zeta - \omega^2 \mathrm{m}\left(\gamma_2 L - \gamma_1 L\right)\int_{\gamma_1}^{\gamma_2} v(\zeta)y(\zeta)\mathrm{d}\zeta = 0. \tag{14}$$

For convenience of analysis, the following nondimensional parameters are also introduced:

$$\gamma = \gamma_2 - \gamma_1; \quad \mathrm{M} = \mathrm{m}\gamma L; \quad \lambda = \frac{\mathrm{M}}{\rho \mathrm{A} L}; \quad \eta = \frac{e_0 a}{L}; \quad \Omega = \sqrt{\frac{\rho \mathrm{A} L^4}{\mathrm{EI}}}. \tag{15}$$

Then, one gets:

$$\int_0^1 \frac{\partial^2 v(\zeta)}{\partial\zeta^2}\frac{\partial^2 y(\zeta)}{\partial\zeta^2}\mathrm{d}\zeta + \omega^2\eta^2\Omega^2\int_0^1 v(\zeta)\frac{\partial^2 y(\zeta)}{\partial\zeta^2}\mathrm{d}\zeta -$$
$$\omega^2\Omega^2\int_0^1 v(\zeta)y(\zeta)\mathrm{d}\zeta - \omega^2\lambda\Omega^2\int_{\gamma_1}^{\gamma_2} v(\zeta)y(\zeta)\mathrm{d}\zeta = 0, \tag{16}$$

and the frequency ω^2 can be written down, putting $\mathrm{y}(\zeta) = \mathrm{v}(\zeta)$, as:

$$\omega^2 = \frac{\int_0^1 \frac{\partial^2 v(\zeta)}{\partial\zeta^2}\frac{\partial^2 v(\zeta)}{\partial\zeta^2}\mathrm{d}\zeta}{\Omega^2\int_0^1 v^2(\zeta)\mathrm{d}\zeta + \Omega^2\lambda\int_{\gamma_1}^{\gamma_2} v^2(\zeta)\mathrm{d}\zeta - \eta^2\Omega^2\int_0^1 v(\zeta)\frac{\partial^2 v(\zeta)}{\partial\zeta^2}\mathrm{d}\zeta}. \tag{17}$$

The equation (13) should be satisfied by different boundary conditions analyzed in detail in the numerical examples section.

3. Approximate fundamental frequency and numerical example

In this section, the fundamental frequency induced by the attached distributed biomolecules is studied.

Here, an alternative approximate method is presented to derive calibration constants for an explicit relationship between the relative frequency shift and added distributed mass. For this purpose, integral expressions of calibration parameters are given and their values are used to derive the fundamental

natural frequency. Finally, defining the frequency shift Δf as the difference between the fundamental frequencies of single-walled carbon nanotube with and without the attached distributed mass, which gives aid as index to assess qualitatively the vibrational behaviour of the nanosensor, the relative frequency shift is calculated and then, it is possible to determine the non dimensional mass expression.

The fundamental natural frequency expression is determined for clamped-free (C-F), clamped-clamped (C-C), simply-supported (S-S), clamped-supported (C-S) and clamped-sliding (C-Sl) nanosensors and mass identification formulae are derived in terms of the frequency shift. Numerical results are illustrated and compared with some results of literature. In the numerical analyses, the effects of the nonlocal parameter, mass and position of the biomolecules on the natural frequency shift of the nanosensor are evaluated.

Table 1 shows the material and geometrical properties of the single-walled carbon nanotube, so as deduced from [33], which will be used throughout all subsequent numerical examples.

SWCNT properties	Symbol	Value	Unit
Cross section area	A	$7.85\ 10^{-19}$	m^2
Radius	R	$0.5\ 10^{-9}$	m
Length	L	$9\ 10^{-9}$	m
Moment of inertia	I	$4.91\ 10^{-38}$	m^4
Density	ρ	2300	Kg/m^3
Young's modulus	E	$1000\ 10^9$	Pa

Table 1: Geometrical and material properties of the single-walled nanotube.

3.1. Clamped-Free nanosensor: approximate fundamental frequency

Firstly, let us consider the value of the first mode of free vibration of a cantilevered nanosensor in the absence of nonlocal effects and added mass:

$$v(\zeta) = (\mathrm{Cosh}(1.8751\zeta) - \mathrm{Cos}(1.8751\zeta)) - \frac{(\mathrm{Sinh}(1.8751) - \mathrm{Sin}(1.8751))}{(\mathrm{Cosh}(1.8751) + \mathrm{Cos}(1.8751))}(\mathrm{Sinh}(1.8751\zeta) - \mathrm{Sin}(1.8751\zeta)) \quad (18)$$

Other choices are obviously possible: for example it is certain that using free vibration modes of nonlocal beams will lead to more precise values.

Nevertheless, the proposed choice seems to be a convenient balance between precision and simplicity.

Substituting the equation (18) into equation (17) the following integrals I_1 and I_3 can be obtained as:

$$I_1 = \int_0^1 v^2(\zeta)\mathrm{d}\zeta = 1; \quad I_3 = \int_0^1 \frac{\partial^2 v(\zeta)}{\partial \zeta^2}\frac{\partial^2 v(\zeta)}{\partial \zeta^2}\mathrm{d}\zeta = 12.3623; \tag{19}$$

For the case of distributed added mass of abscissae $\gamma_2 - \gamma_1$, the integral I_2 can be expressed as:

$$I_2 = \frac{1}{\gamma_2 - \gamma_1}\int_{\gamma_1}^{\gamma_2} v^2(\zeta)\mathrm{d}\zeta; \quad 0 \leq \gamma_1 \leq 1; \quad 0 \leq \gamma_2 \leq 1 \text{ and } \gamma_1 \neq \gamma_2 \tag{20}$$

so as calculated in Table 1 of the paper [31].
We define a fourth integral in order to take into account the nonlocal effects as:

$$I_4 = \int_0^1 v(\zeta)\frac{\partial^2 v(\zeta)}{\partial \zeta^2}\mathrm{d}\zeta = 0.858264; \tag{21}$$

The fundamental natural frequency for attached distributed mass can be deduced from equations ((17),(19),(20) and (21)) in terms of these four integrals as:

$$f_{\mathrm{n1}} = \frac{\omega}{2\pi} = \frac{\beta}{2\pi}\sqrt{\frac{I_3}{I_1 + \lambda I_2 - \eta^2 I_4}} \tag{22}$$

where $\beta = \frac{1}{\Omega}$.

Finally, dividing the above equation for I_1, an alternative version of the first natural frequency can be obtained as

$$f_{\mathrm{n1}} = \frac{\beta}{2\pi}\frac{C_k}{\sqrt{1 + \lambda C_m - \eta^2 C_{\mathrm{n1}}}} \tag{23}$$

where C_k, C_m and C_{n1} are the so-called calibration constants, so defined:

$$C_k = \sqrt{\frac{I_3}{I_1}} = 3.5160; \quad C_{\mathrm{n1}} = \frac{I_4}{I_1} = 0.858264; \quad C_m = \frac{I_2}{I_1} \tag{24}$$

As can be seen the stiffness C_k calibration constant is equivalent to the value reported in Table 1 of the paper [31] as well as the values of the mass C_m calibration constant obtained for different values of γ.

It is possible to calculate the frequency shift of the biosensor as:

$$\Delta \mathrm{f} = f_0 - f_{\mathrm{n1}} \tag{25}$$

where f_0 is the natural frequency of the nanotube without added mass and neglecting the nonlocal effect.

The natural frequency value f_0 is given by:

$$f_0 = \frac{1}{2\pi} C_k \beta \tag{26}$$

from this, the equation (25) becomes:

$$\Delta \mathrm{f} = f_0 - f_{\mathrm{n1}} = f_0 \left(1 - \frac{1}{\sqrt{1 + \lambda C_m - \eta^2 C_{\mathrm{n1}}}} \right) \tag{27}$$

The relative frequency shift can therefore be expressed as:

$$\frac{\Delta \mathrm{f}}{f_0} = \left(1 - \frac{1}{\sqrt{1 + \lambda C_m - \eta^2 C_{\mathrm{n1}}}} \right) \tag{28}$$

from which the value of the added mass M can be easily obtained as:

$$\mathrm{M} = \frac{\rho \mathrm{A} L}{C_m \left(1 - \frac{\Delta \mathrm{f}}{f_0} \right)^2} - \frac{\rho A L}{C_m} + \frac{\eta^2 \rho \mathrm{A} L C_{\mathrm{n1}}}{C_m} \tag{29}$$

This is the general equation which relates the added mass and the frequency shift in the presence of the nonlocal effect and using the calibration constants. These calibration constants change depending on the position of the added mass and boundary conditions. Their values have been calculated previously.

3.1.1. Clamped-free nanosensor: numerical example

In this numerical case, one assumes a fixed location of attached mass, at the free end, and setting $\gamma = \gamma_2 - \gamma_1$ and γ_2=1, it is possibile to increase the value of γ varying γ_1. The nondimensional mass is so defined:

$$\lambda = \frac{\mathrm{m}\,(1-\gamma_1)\,L}{\rho \mathrm{A} L} \tag{30}$$

The relative frequency shift, so as deduced from the work of Adikari and Chowdhury [31] for η=0, is given by the following expression:

$$\frac{\Delta \mathrm{f}}{f_0} = 1 - \frac{1}{\sqrt{1 + C_m \lambda}} \tag{31}$$

where C_m is mass calibration constant which is a function of the length of the attached distributed mass γ as shown in Table 1 of the paper [31].

γ	$\Delta f/f_0$ [31]	$\Delta f/f_0$ [35]	$\Delta f/f_0$
0.1	0.13853	0.13908	0.13854
0.2	0.20947	0.21007	0.20947
0.3	0.24918	0.24956	0.24918
0.4	0.27163	0.27180	0.27163
0.5	0.28375	0.28380	0.28375
0.6	0.28965	0.28966	0.28965
0.7	0.29206	0.29206	0.29206
0.8	0.29277	0.29277	0.29277

Table 2: Numerical comparison with the papers [31] and [35].

Table 2 shows a numerical comparison among [31], [35] and the present approximate approach. The first column gives the fundamental natural frequency in the absence of nonlocal effects. As can be easily observed, with the increase in the value of γ, the relative frequency shift value deduced from the approximate formula approaches the value obtained from the exact solution [35]; whereas for the values of equal to 0.7 and 0.8, the approximate and exact relative frequency shift values coincide.

In Table 3, the first resonant frequency f_1 (exact [35] and present method (p.m.)) value is reported for the dimensionless coefficients of the length γ that varies between 0 and 0.9 and the non local effect values η [0, 0.1, 0.3, 0.5].

The first value of the natural frequency, reported in Table 3 and for γ=0, can be compared with those obtained from the formula (163) in the article

γ	$\eta = 0$	$\eta = 0.1$	$\eta = 0.3$	$\eta = 0.5$
0 [33]	3.60268	3.61834	3.75909	4.18895
0 [p.m.]	3.60268	3.61826	3.75046	4.06512
0.1 [35]	3.10162	3.11245	3.20756	3.46665
0.1 [p.m.]	3.10361	3.11355	3.19659	3.38478
0.2 [35]	2.84585	2.85418	2.926	3.10933
0.2 [p.m.]	2.84804	2.85571	2.91937	3.06062
0.3 [35]	2.70360	2.71057	2.77009	2.91661
0.3 [p.m.]	2.70498	2.71155	2.76587	2.88509
0.4 [35]	2.62348	2.62970	2.68251	2.80985
0.4 [p.m.]	2.62412	2.63011	2.67959	2.78757
0.5 [35]	2.58023	2.58605	2.63527	2.75263
0.5 [p.m.]	2.58045	2.58615	2.63315	2.73539
0.6 [35]	2.55911	2.56473	2.6122	2.72473
0.6 [p.m.]	2.55916	2.56472	2.61055	2.71007
0.7 [35]	2.55048	2.55602	2.60277	2.71335
0.7 [p.m.]	2.55050	2.55602	2.60135	2.69979
0.8 [35]	2.54791	2.55342	2.59996	2.70995
0.8 [p.m.]	2.54792	2.55341	2.59862	2.69673
0.9 [35]	2.54749	2.55301	2.59951	2.70941
0.9 [p.m.]	2.54751	2.55299	2.59817	2.69624

Table 3: First exact [35] and approximate (p.m.) fundamental natural frequency (x 10^{10}) f_{n1} for a clamped-free nanotube for various values of the non-dimensional length γ of the added mass and for increasing values of the nonlocal nondimensional coefficient η.

[33]. As one can see, the results are coincident. For the other numerical results, the following considerations apply:

- if γ increases, the first natural frequency value decreases;

- if the nonlocal effect non-dimensional parameter increases, the first natural frequency value increases.

In Figure 2, the normalized added mass $\lambda = \frac{\mathrm{M}}{\rho \mathrm{A} L}$ is plotted against the relative frequency shift equation (28) and the four curves refer to four different η values: $\eta = 0$ (without nonlocal effects), $\eta = 0.1$, $\eta = 0.2$ and $\eta = 0.3$. As it can be seen, the relative frequency shift decreases for increasing values of the nonlocal coefficient η, whereas if the attached mass increases the relative frequency shift decreases greatly and for $\lambda \simeq 0.7$ it assumes a stable trend.

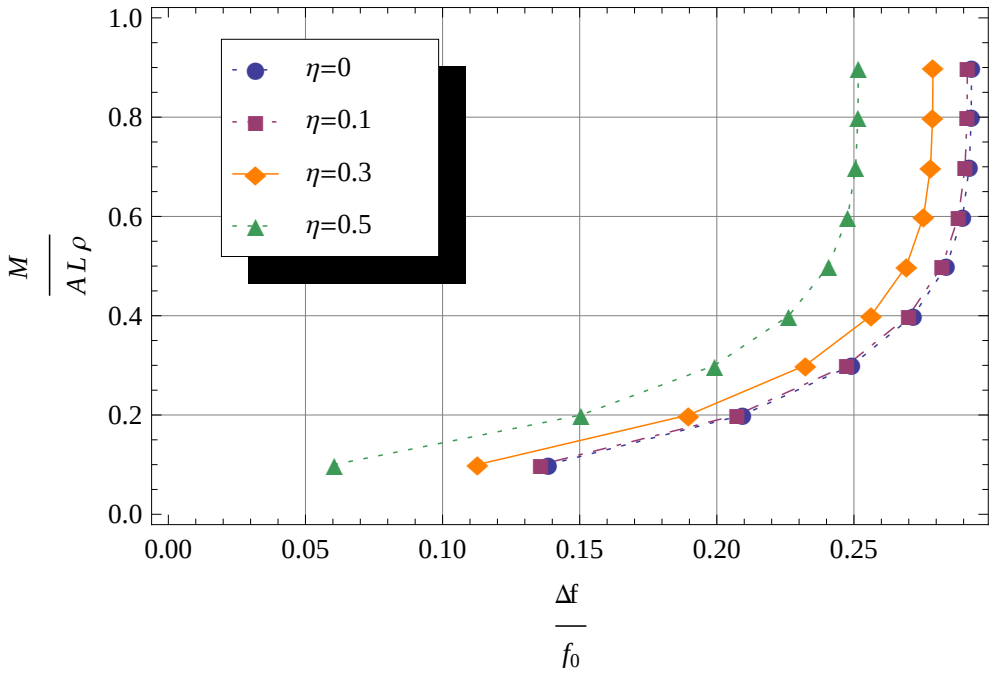

Figure 2: Clamped-free nanosensor: the normalized added mass $\lambda = \frac{M}{\rho A L}$ is plotted against the relative frequency shift. The four curves refer to four different η values: η=0 (without nonlocal effect), η=0.1, η=0.3, η=0.5.

3.2. Clamped-Clamped nanosensor: approximate fundamental frequency

Here, a clamped-clamped nanosensor is considered. The first mode shape of vibration can be expressed as:

$$v(\zeta) = (\mathrm{Cosh}(4.73\zeta) - \mathrm{Cos}(4.73\zeta)) - \frac{(\mathrm{Cosh}(4.73) - \mathrm{Cos}(4.73))}{(\mathrm{Sinh}(4.73) - \mathrm{Sin}(4.73))}(\mathrm{Sinh}(4.73\zeta) - \mathrm{Sin}(4.73\zeta)) \tag{32}$$

The integrals of equation (17) become:

$$I_1 = \int_0^1 v^2(\zeta)\mathrm{d}\zeta = 1; \quad I_3 = \int_0^1 \frac{\partial^2 v(\zeta)}{\partial\zeta^2}\frac{\partial^2 v(\zeta)}{\partial\zeta^2}\mathrm{d}\zeta = 500.534;$$
$$I_4 = \int_0^1 v(\zeta)\frac{\partial^2 v(\zeta)}{\partial\zeta^2}\mathrm{d}\zeta = -12.3025. \tag{33}$$

For the case of distributed added mass of length $\gamma_2 - \gamma_1$, the integral I_2 can be obtained, as into equation (19), and the two calibration constants can be derived as:

$$C_k = \sqrt{\frac{I_3}{I_1}} = 22.3725; \quad C_{\mathrm{n1}} = \frac{I_4}{I_1} = -12.3024 \tag{34}$$

3.2.1. Clamped-clamped nanosensor: numerical example

For the numerical example, the nanosensor, carrying a biomolecules of mass m placed symmetrically about the center, is considered. For example, for γ=0.2, the mass occupies a space between γ_1=0.4 to γ_2=0.6. In Table 4 the corresponding exact and approximate values of the first natural frequency, so as deduced to equation (23), are reported.

It can be seen that with the increase in the value of the added mass and the nonlocal effect parameter, the value of the fundamental natural frequency decreases. In Figure 3, the nondimensional ratio $\frac{\mathrm{M}}{\rho \mathrm{A} L}$ is plotted against the relative frequency shift equation (31) and the four curves refer to four different values of the nonlocal coefficient η (0, 0.1, 0.3, 0.5). It is interesting to note that the relative frequency shify increases for increasing values of the added distributed mass and this trend becomes less sensitive to an change in the mass or location of the attached biomolecules and in particular starting from a λ value equal to about 0.6. As it can be noted, for λ >0.6 the relative frequency shift trend becomes constant. In addition, with increasing values of the nonlocal η parameter, clearly the relative frequency shift increases; whereas for higher values of the nonlocal coefficient η, the influence of the attached mass on the relative frequency shift is less significant.

3.3. Simple-supported nanosensor: approximate fundamental frequency

In the following case, the simple-supported nanosensor is considered and the corresponding mode shape of vibration can be expressed as:

γ	$\eta = 0$	$\eta = 0.1$	$\eta = 0.3$	$\eta = 0.5$
0 [35]	2.29249	2.16295	1.57321	1.12623
0 [p.m.]	2.29241	2.1632	1.5792	1.13552
0.1 [35]	2.05034	1.95552	1.48704	1.09327
0.1 [p.m.]	2.05150	1.95734	1.49354	1.10239
0.2 [35]	1.88440	1.80983	1.41968	1.06569
0.2 [p.m.]	1.77340	1.71081	1.37047	1.04452
0.3 [35]	1.77507	1.71302	1.37612	1.05256
0.3 [p.m.]	1.70191	1.64646	1.33706	1.02968
0.4 [35]	1.70284	1.64783	1.34164	1.03688
0.4 [p.m.]	1.65879	1.60746	1.31638	1.02038
0.5 [35]	1.65913	1.60813	1.31994	1.02677
0.5 [p.m.]	1.63550	1.58637	1.30515	1.01533
0.6 [35]	1.63555	1.58663	1.30798	1.02111
0.6 [p.m.]	1.62851	1.58005	1.30185	1.01312
0.7 [35]	1.62501	1.57700	1.30257	1.01853
0.7 [p.m.]	1.62165	1.57511	1.29925	1.01243
0.8 [35]	1.62159	1.57387	1.30081	1.01768
0.8 [p.m.]	1.62106	1.57332	1.29832	1.01232
0.9 [35]	2.54749	2.55301	2.59951	2.70941
0.9 [p.m.]	1.62100	1.57333	1.30050	1.01754

Table 4: First exact [35] and approximate (p.m.) fundamental natural frequency (x 10^{10}) f_{n1} for a clamped-clamped nanotube for various values of the non-dimensional length γ of the added mass and for increasing values of the nonlocal nondimensional coefficient η.

$$v(\zeta) = \mathrm{Sin}(\pi\zeta). \tag{35}$$

Starting from equation (22) the integrals become:

$$\begin{aligned} I_1 &= \int_0^1 v^2(\zeta)\mathrm{d}\zeta = \frac{1}{2}; \quad I_3 = \int_0^1 \frac{\partial^2 v(\zeta)}{\partial\zeta^2}\frac{\partial^2 v(\zeta)}{\partial\zeta^2}\mathrm{d}\zeta = \frac{\pi^4}{2}; \\ I_4 &= \int_0^1 v(\zeta)\frac{\partial^2 v(\zeta)}{\partial\zeta^2}\mathrm{d}\zeta = -\frac{\pi^2}{2}; \end{aligned} \tag{36}$$

and the two calibration constants, mass-indipendent, are:

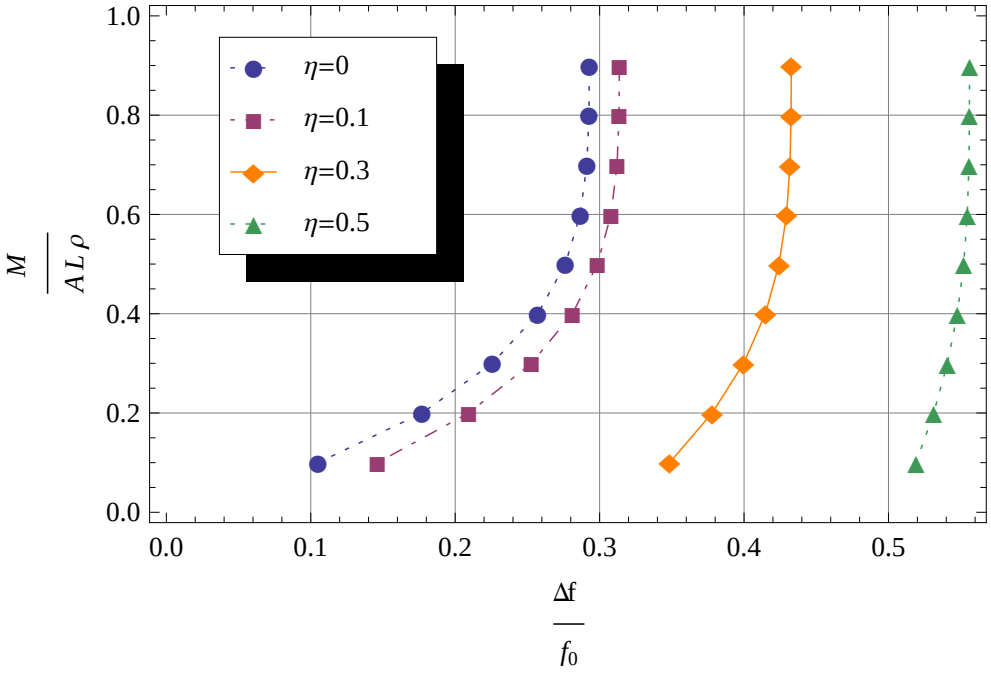

Figure 3: Clamped-clamped nanosensor: the normalized added mass $\lambda = \frac{\mathrm{M}}{\rho \mathrm{A} L}$ is plotted against the relative frequency shift. The four curves refer to four different η values: η=0 (without nonlocal effect), η=0.1, η=0.3, η=0.5.

$$C_k = \sqrt{\frac{I_3}{I_1}} = \pi^2; \quad C_{\mathrm{n1}} = \frac{I_4}{I_1} = -\pi^2. \tag{37}$$

3.3.1. Simple-supported nanosensor: numerical example

Table 5 gives a comparison among the exact and approximate values of the first fundamental natural frequency - so as deduced from eq. (22) - for the simple-supported nanosensor case carrying an attached biomolecules with mass placed symmetrically about center of the nanosensor. As it can be see, the exact and approximate results are coincident; in addition, it is clear from Table 5 that the fundamental natural frequency decreases when the added mass and the nondimensional nonlocal effect coefficient increase. More precisely, Figure 4 shows that with increasing the normalized added mass increases the relative frequency shift increases; as pointed out before, this trend becomes less sensitive to an change in the location of the attached

γ	$\eta = 0$	$\eta = 0.1$	$\eta = 0.3$	$\eta = 0.5$
0 [35]	10.1129	9.64802	7.35945	5.43094
0 [p.m.]	1.01129	9.64802	7.35945	5.43094
0.1 [35]	9.23640	8.87827	7.00047	5.28184
0.1 [p.m.]	9.23810	8.87967	7.00091	5.28196
0.2 [35]	8.5832	8.29364	6.70323	5.15073
0.2 [p.m.]	8.58664	8.29655	6.70427	5.15102
0.3 [35]	8.09970	7.85503	6.46528	5.04043
0.3 [p.m.]	8.10327	7.85812	6.46648	5.04079
0.4 [35]	7.74741	7.53245	6.28171	4.95195
0.4 [p.m.]	7.75004	7.53474	6.28266	4.95224
0.5 [35]	7.49823	7.30279	6.14649	4.88483
0.5 [p.m.]	7.49968	7.30407	6.14705	4.88501
0.6 [35]	7.33083	7.14784	6.05314	4.83752
0.6 [p.m.]	7.33142	7.14837	6.05337	4.83760
0.7 [35]	7.22794	7.05235	5.99475	4.80753
0.7 [p.m.]	7.22810	7.05249	5.99482	4.80755
0.8 [35]	7.17408	7.00229	5.96390	4.79156
0.8 [p.m.]	7.17410	7.00231	5.96390	4.79157
0.9 [35]	7.15385	6.98347	5.95225	4.78552
0.9 [p.m.]	7.15385	6.98347	5.95225	4.78552

Table 5: First exact [35] and approximate (p.m.) fundamental natural frequency (x 10^{10}) f_{n1} for a simple-supported nanotube for various values of the non-dimensional length γ of the added mass and for increasing values of the nonlocal nondimensional coefficient η.

biomolecules and in particular starting from a λ value equal to about 0.8. Moreover, the relative frequency shift increases if the nondimensional nonlocal effect η increases.

3.4. Clamped-supported nanosensor: approximate fundamental frequency

Here the clamped-supported nanosenor is considered and the following approximate function for the first mode of vibration is assumed:

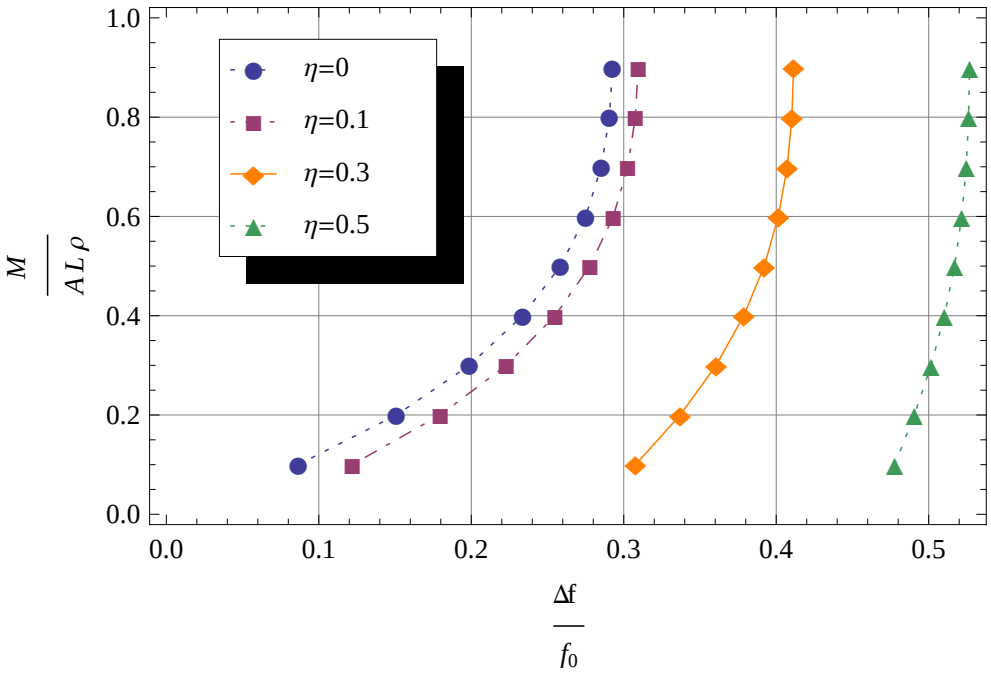

Figure 4: Simple-supported nanosensor: the normalized added mass $\lambda = \frac{\mathrm{M}}{\rho \mathrm{A} L}$ is plotted against the relative frequency shift. The four curves refer to four different η values: η=0 (without nonlocal effect), η=0.1, η=0.3, η=0.5.

$$v(\zeta) = (\mathrm{Cosh}(3.92660231\zeta) - \mathrm{Cos}(3.92660231\zeta)) - \frac{(\mathrm{Cosh}(3.92660231) - \mathrm{Cos}(3.92660231))}{(\mathrm{Sinh}(3.92660231) - \mathrm{Sin}(3.92660231))}(\mathrm{Sinh}(3.92660231\zeta) - \mathrm{Sin}(3.92660231\zeta)) \tag{38}$$

Using equation (22) the integrals I_1, I_3 and I_4 can be obtained as:

$$I_1 = \int_0^1 v^2(\zeta)\mathrm{d}\zeta = 1; \quad I_3 = \int_0^1 \frac{\partial^2 v(\zeta)}{\partial \zeta^2}\frac{\partial^2 v(\zeta)}{\partial \zeta^2}\mathrm{d}\zeta = 273.721;$$
$$I_4 = \int_0^1 v(\zeta)\frac{\partial^2 v(\zeta)}{\partial \zeta^2}\mathrm{d}\zeta = -11.5125; \tag{39}$$

Using these integrals, the calibration factors, mass-indipendent, can be derived as:

$$C_k = \sqrt{\frac{I_3}{I_1}} = 15.4182; \quad C_{\mathrm{n1}} = \frac{I_4}{I_1} = -11.5125. \tag{40}$$

3.4.1. Clamped-supported nanosensor: numerical example

In Table 6, the first natural frequency values of clamped-supported nanosensor are reported. As it can note, the difference among the exact and approximated value decreases with increasing the length of attached distributed mass and it stabilizes for $\lambda \simeq 0.8$. In addition the first frequency valued decreases with increasing the nondimensional nonlocal effect coefficient η. Figure 5 shows a comparison of the exact value and its approximation for a clamped-supported nanosensor, where the nonlocal parameter is chosen as $\eta = 0,\ 0.1,\ 0.3,\ 0.5$. From Figure 5, one notes that the clamped-supported nanosensor behaviour is close to the previous numerical examples behaviour.

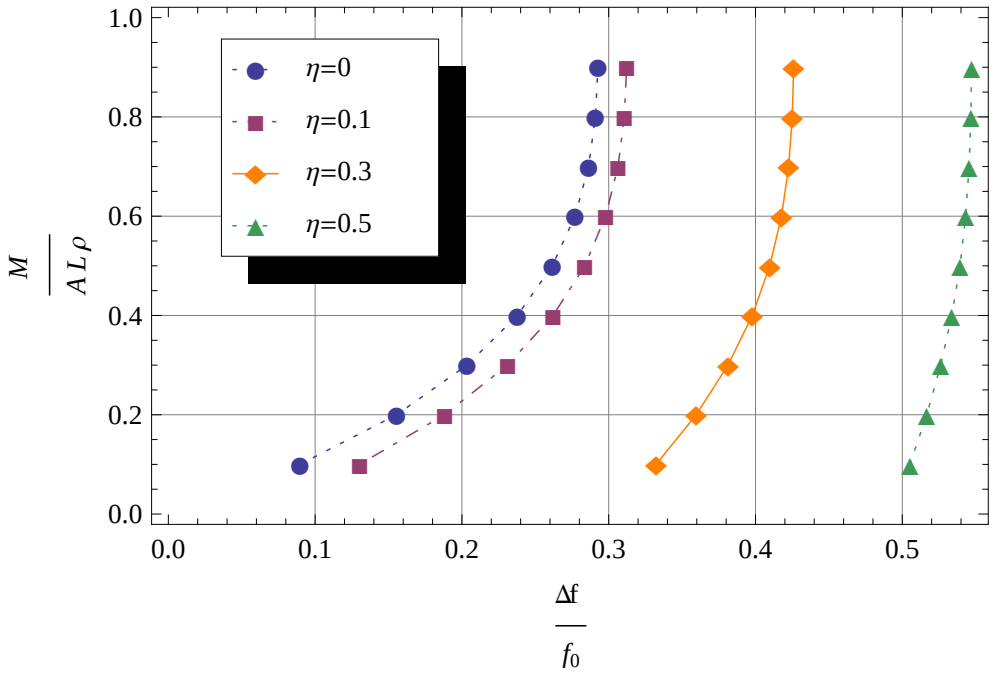

Figure 5: Clamped-supported: the normalized added mass $\lambda = \frac{\mathrm{M}}{\rho \mathrm{AL}}$ is plotted against the relative frequency shift. The four curves refer to four different η values: η=0 (without nonlocal effect), η=0.1, η=0.3, η=0.5.

γ	$\eta = 0$	$\eta = 0.1$	$\eta = 0.3$	$\eta = 0.5$
0 [35]	1.57983	1.49591	1.10427	0.79756
0 [p.m.]	1.57983	1.49606	1.10716	0.80223
0.1 [35]	1.43735	1.37351	1.05294	0.77788
0.1 [p.m.]	1.43811	1.37406	1.05488	0.78166
0.2 [35]	1.33264	1.28141	1.01018	0.76043
0.2 [p.m.]	1.33416	1.28255	1.01173	0.76361
0.3 [35]	1.25682	1.21361	0.97617	0.74576
0.3 [p.m.]	1.25839	1.21481	0.97747	0.74855
0.4 [35]	1.20301	1.16493	0.95030	0.73409
0.4 [p.m.]	1.20416	1.16581	0.951340	0.73665
0.5 [35]	1.16601	1.13120	0.93162	0.72536
0.5 [p.m.]	1.16665	1.13167	0.93256	0.72780
0.6 [35]	1.14188	1.10907	0.91901	0.71932
0.6 [p.m.]	1.14214	1.10926	0.91990	0.72173
0.7 [35]	1.12749	1.09583	0.91131	0.71555
0.7 [p.m.]	1.12755	1.09588	0.91223	0.71801
0.8 [35]	1.12017	1.08908	0.90733	0.71358
0.8 [p.m.]	1.12018	1.08910	0.90831	0.71610
0.9 [35]	1.11749	1.08661	0.90586	0.71285
0.9 [p.m.]	1.11749	1.08663	0.90688	0.71539

Table 6: First exact [35] and approximate (p.m.) fundamental natural frequency (x 10^{11}) f_{n1} for a clamped-supported nanotube for various values of the non-dimensional length γ of the added mass and for increasing values of the nonlocal nondimensional coefficient η.

3.5. Clamped-sliding nanosensor: approximate fundamental frequency

Finally, the clamped-sliding (C-Sl) nanosensor case is considered. For the C-Sl single-walled carbon nanotube the following vibration mode shape function is given:

$$v(\zeta) = \frac{\mathrm{Sin}(2.36502037\zeta) - (\mathrm{Cos}(2.36502037\zeta)(-\mathrm{Cos}(2.36502037) + \mathrm{Cosh}(2.36502037)))}{(\mathrm{Sin}(2.36502037) + \mathrm{Sinh}(2.36502037))} - \frac{(\mathrm{Cos}(2.36502037) - (\mathrm{Cosh}(2.36502037))\mathrm{Cosh}(2.36502037\zeta))}{(\mathrm{Sin}(2.36502037) + \mathrm{Sinh}(2.36502037)) - \mathrm{Sinh}(2.36502037\zeta)} \tag{41}$$

Using the equation (22) the integrals I_1, I_3 and I_4 can be obtained as:

$$I_1 = \int_0^1 v^2(\zeta)\mathrm{d}\zeta = 1.03594; \quad I_3 = \int_0^1 \frac{\partial^2 v(\zeta)}{\partial\zeta^2}\frac{\partial^2 v(\zeta)}{\partial\zeta^2}\mathrm{d}\zeta = 32.4095;$$
$$I_4 = \int_0^1 v(\zeta)\frac{\partial^2 v(\zeta)}{\partial\zeta^2}\mathrm{d}\zeta = -3.18618; \tag{42}$$

and the calibration factors are:

$$C_k = \sqrt{\frac{I_3}{I_1}} = 5.59332; \quad C_{\mathrm{n1}} = \frac{I_4}{I_1} = -3.07565; \tag{43}$$

γ	$\eta = 0$	$\eta = 0.1$	$\eta = 0.3$	$\eta = 0.5$
0 [35]	5.73122	5.6450	5.06895	4.29809
0 [p.m.]	5.73120	5.64506	5.07205	4.30917
0.1 [35]	5.52669	5.44970	4.92848	4.21361
0.1 [p.m.]	5.52792	5.45049	4.92952	4.22073
0.2 [35]	5.33559	5.26656	4.79368	4.13030
0.2 [p.m.]	5.33928	5.26942	4.79435	4.13495
0.3 [35]	5.15336	5.09130	4.66162	4.04631
0.3 [p.m.]	5.15915	5.09604	4.66266	4.04957
0.4 [35]	4.98413	4.92715	4.53225	3.96326
0.4 [p.m.]	4.98413	4.92715	4.53225	3.96326
0.5 [35]	4.80683	4.75638	4.40097	3.87329
0.5 [p.m.]	4.81297	4.76160	4.40240	3.87555
0.6 [35]	4.64135	4.59580	4.27242	3.78460
0.6 [p.m.]	4.64603	4.59978	4.27357	3.78679
0.7 [35]	4.48181	4.44063	4.14628	3.69561
0.7 [p.m.]	4.48469	4.44305	4.14700	3.69789
0.8 [35]	4.32949	4.29221	4.02401	3.60766
0.8 [p.m.]	4.33080	4.29326	4.02441	3.61018
0.9 [35]	4.18592	4.15208	3.90723	3.52222
0.9 [p.m.]	14.15230	4.15230	3.90762	3.52515

Table 7: First exact [35] and approximate (p.m.) fundamental natural frequency (x 10^{10}) f_{n1} for a clamped-sliding nanotube for various values of the non-dimensional length γ of the added mass and for increasing values of the nonlocal nondimensional coefficient η.

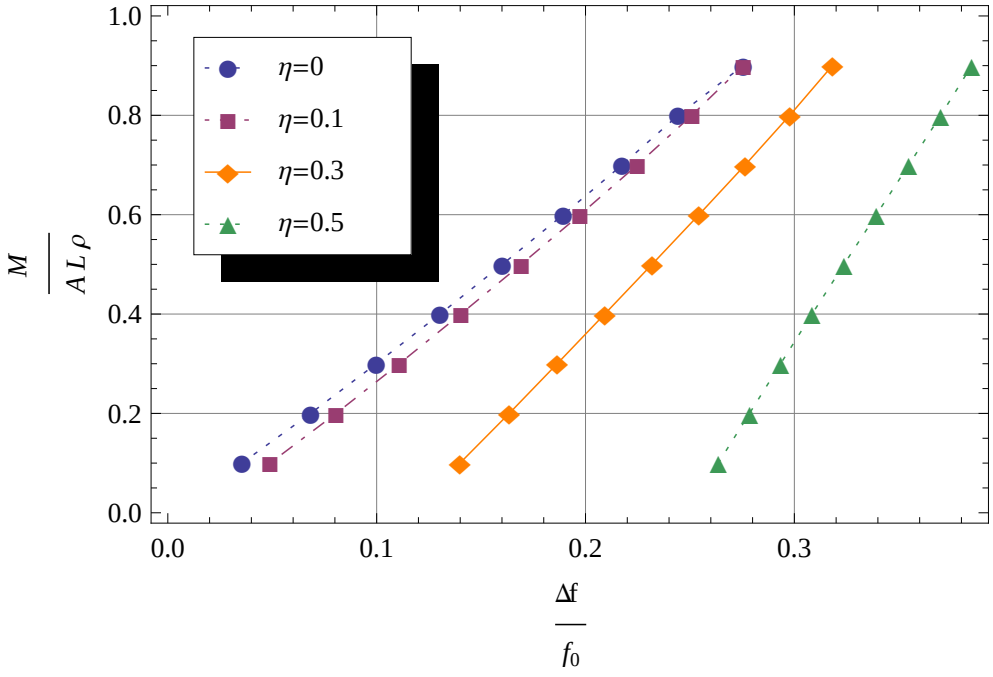

Figure 6: Clamped-sliding nanosensor: the normalized added mass $\lambda = \frac{M}{\rho A L}$ is plotted against the relative frequency shift. The four curves refer to four different η values: η=0 (without nonlocal effect), η=0.1, η=0.3, η=0.5.

3.5.1. Clamped-sliding nanosensor: numerical example

For this numerical case, the first natural frequency values are listed in Table 7; as it can be seen the first natural frequency value decreases for increasing values of the nonlocal η parameter. However, it is interesting to note that the difference among the exact and approximate value is greater than the other numerical cases and this is mainly due to the approximate function considered. In addition, the four curves in Figure 6 show that the influence of added distributed mass on the relative frequency shift value becomes stronger and the obtained function has a linear behaviour. This also implies that for a clamped-sliding nanosensor it has an opposite trend to the above numerical examples.

Conclusions

In the present note, the natural frequency of SWCNT based mass-sensor, carrying a distributed mass located in a generic position, has been inves-

tigated. The nonlocal Euler-Bernoulli beam theory has been used and the influence of the nonlocal coefficient on the first natural frequency value has been evaluated. The fundamental natural frequency close-form expression has been derived and the corresponding shift frequency have been calculated. Numerical results for different boundary conditions have been performed in order to evaluate the effect of the nonlocal coefficient. The obtained results can be employed to find the distributed added mass: from natural frequency value, in absence of mass and nonlocal effect, and the natural frequency value, in presence of the mass and nonlocal effect, it is possibile to derive the relative frequency shift and from theoretical curves calculate the normalized added mass $\frac{\mathrm{M}}{\rho \mathrm{A} L}$ for relative frequency shift.
The conclusions are drawn as follows:

a) The clamped-free nanosensor case has an opposite trend to the other boundary conditions because:
- if the nonlocal effect nondimensional η increases, the first natural frequency value increases.
- if the nondimensional added mass m increases, the first natural frequency value decreases;
whereas the Clamped-Clamped, Simple supported, Clamped-supported e Clamped-sliding cases hold the following observations:
- if the nondimensional added mass λ increases, the first natural frequency value decreases;
- if the nonlocal effect nondimensional η parameter increases, the first natural frequency value decrease.

b) Finally, comparing the approximate results of the present paper and the exact results given in [35], the different behaviour exhibited by the results depends on the approximate function chosen.

The present approach can be applied to analyze the dinamic behaviour of multi-walled carbon nanotubes (MWCNTs) and in the case of nanotubes based upon the Timoshenko theory.

Aknowledgments

The authors would like to thank the anonymous reviewers for their constructive comments and precious suggestions on an earlier version of the paper.

References

[1] S. Iijima, Helical microtubules of graphitic carbon, Nature (London) 354 (1991) 56-58.

[2] J.P. Salvetat, J.-M. Bonard, N.H. Thomson, A.J. Kulik, L. Forro, W. Benoit, L. Zuppiroli, Mechanical properties of carbon nanotubes, Appl. Phys. A 69 (1999) 255-260.

[3] E.T. Thostenson, Z.R., T.W. Chou, Advances in the science and technology of carbon nanotubes and their composites: a review, Comp. Sci. and Tech. 61 (13) (2001) 1899-1912.

[4] B.G. Demczyk , Y.M Wang, Y.M. Wang , J. Cumings , M. Hetman , W. Han , A. Zettl , R.O. Ritchie, Direct mechanical measurement of the tensile strength and elastic modulus of multiwalled carbon nanotubes, Mat. Sci. and Eng. A 334 (1-2) (2002) 173-178.

[5] P.G. Collins, P. Avouris, Nanotubes for electronics, Scientific American 283(6) (2000) 62-69.

[6] D.H. Wu, W.T. Chien, C.S. Chen and H.H.Chen, Resonant frequency analysis of fixed-free single-walled carbon Nanotube-Based Mass Sensor, Sensors and Actuators A 126 (2006) 117-121.

[7] A.Y. Joshi, S.C. Sharma, S.P. Harsha, Dynamic analysis of a clamped wavy single walled carbon nanotube based nanomechanical sensors, J. of Nanotech. in Eng. and Medicine 1 (2010) 031007-031014.

[8] I. Mehdipour, A. Barari, G. Domairry, Application of a cantilevered SWCNT with mass at the tip as a nanomechanical sensor, Comp. Mat. Sci., 50 (2011) 1830-1833.

[9] S.K. Georgantzinos, N.K. Anifantis, Carbon nanotube-based resonant nanomechanical sensors: a computational investigation of their behavior, Physica E, 42 (5) (2010) 1795-1801.

[10] I. Elishakoff, C. Versaci, G. Muscolino, Clamped-Free double-walled carbon nanotube-based mass sensor, Acta Mechanica, 219 (2011) 29-43.

[11] I. Elishakoff, C. Versaci, G. Muscolino, Effective stiffness and effective mass of the double-walled carbon nanotube sensor, Journal of Nanotechnology in Engineering and Medicine, 2 (1) (2011) 011008.

[12] I. Elishakoff, N. Challamel, C. Soret, Y. Bekel and T. Gomez, Virus sensor based on single-walled carbon nanotube: improved theory incorporating surface effects, Philosophical Transactions of the Royal Society A: Mathematical, Physical and Engineering Sciences, 371 (1993) (2013) 20120424.

[13] I. Elishakoff, D. Pentaras, K. Dujat, C. Versaci, G. Muscolino, J. Storch, S. Bucas, N. Challamel, T. Natsuki, Y.Y. Zhang, C.M. Wang and G. Ghyselinck, Carbon Nanotubes and Nano Sensors : Vibrations, Buckling, and Ballistic Impact, ISTE-Wiley, London, (2012).

[14] R. Mateiu, A. Kuhle, R. Marie, A. Boisen, Building a multi-walled carbon nanotube-based mass sensor with the atomic force microscope, Ultramicroscopy, 105 (2005) 233-237.

[15] J.W. Kang, O.K. Kwon, J.H. Lee, Y.G. Choi, H. J. Hwang, Frequency change by inter-walled length difference of double-walled carbon nanotube resonator, Solid State Communications, 149(1): 1574-1577, (2009).

[16] J.W. Kang, O.K. Kwon, H. J. Hwang, Q. Jiang, Resonance frequency distribution of cantilevered (5,5) (10,10) double-walled carbon nanotube with different intertube lengths, Moecular. Simuletion, 37(1) (2011) 18-22.

[17] I. Elishakoff, D. Pentaras, Fundamental natural frequencies of double-walled carbon nanotubes, J. of Sound and Vibration, 322 (2009) 652-664.

[18] A.C. Eringen, On differential equations of non local elasticity and solutions of screw dislocation and surface-waves, J. Appl. Phys. 54 (1983) 4703-4710.

[19] J.N.Reddy, Nonlocal theories for bending, buckling and vibration of beams, Int. J. of Eng. Sci. 45 (2007) 288-307.

[20] J. Peddieson, G.R. Buchanan, R.P. McNitt, Application of nonlocal continuum models to nanotechnology, Int. J. Eng. Sci. 41 (2003) 305-312.

[21] S.A.M. Ghannadpour, B. Mohammadi, J. Fazilati, Bending buckling and vibration problems of nonlocal Euler beams using Ritz method, Composite Structures 96 (2013) 584-589.

[22] S.C. Pradhan, J.K. Phadicar, Bending buckling and vibration analyses of nonhomogeneous nanotubes using GDQ and nonlocal elasticity theory, Struct. Eng. and Mech. an Int. Journal 33 (2) (2009) 193-213.

[23] Q. Wang Q, V.K. Varadan, Vibration of carbon nanotubes studied using nonlocal continuum mechanics, Smart Materials and Structures 15 (2006) 659-666.

[24] M.A. De Rosa, M. Lippiello, Free vibration analysis of DWCNTs using CDM and Rayleigh-Schimdt based on nonlocal Euler-Bernoulli beam theory, The Scientific World Journal, 2014 (2014).

[25] R. Ansari, S. Sahmani, Small scale effect on vibrational response of single-walled carbon nanotubes with different boundary conditions based on nonlocal beam models, Commun.Nonlinear Sci. Numer. Simulat. 17 (2012) 1965-1979.

[26] H.L. Lee, J.C. Hsu, W. J. Chang, Frequency shift of carbon nanotube-based mass sensors using nonlocal elasticity theory, Nanoscale Research Letters 5 (2010) 1774-1778.

[27] M. Aydogdu, S. Filiz, Modeling carbon nanotube-based mass sensors using axial vibration and nonlocal elasticity, Physica E 43 (2001) 1229-1234.

[28] Z.B. Shen, B. Deng, X.F. Li, G.J. Tang, Buckling Instability of Carbon Nanotube Atomic Force Microscope Probe Clamped in an Elastic Medium, ASME J. Nanotechnol. Eng. Med. 2 (2011) 031003.

[29] R. Chowdhury, S. Adhikari, J. Mitchell, Vibrating carbon nanotube based bio-sensor, Physica E 42 (2009) 104-109.

[30] T. Murmu, S. Adhikari, Nonlocal frequency analysis of nanoscale biosensors, Sensor and Actuators A, 173 (2012) 41-48.

[31] S. Adhikari, R. Chowdhury, The calibration of nanotube based bionanosensors, Journal of Applied Physics, 107 (2010) 124322.

[32] M.A. De Rosa, M. Lippiello, Hamilton Principle for SWCN and a modified approach for nonlocal frequency analysis of nanoscale biosensor, Int. J. of Recent Scient. Research, 6 (1) (2015) 2355-2365.

[33] J.N. Reddy, S.D. Pang, Nonlocal continuum theories of beams for the analysis of carbon nanotubes, J. of Appl. Physics, 103 (2008) 023511-26.

[34] N. Challamel, Z. Zhang, C.M. Wang, J.N. Reddy, Q. Wang, T. Michelitsch, B. Collet, On nonconservativeness of Eringen's nonlocal elasticity in beam mechanics: correction from a discrete-based approach, Arch. Appl. Mech, 84 (2014) 1275-1292.

[35] M.A. De Rosa, C. Franciosi, M. Lippiello, M.T. Piovan, Nonlocal frequency analysis of nanosensors with attached distributed biomolecules with different boundary conditions, Mecanica Computacional, 33 (23) (2014) 1529-1541.

Appendix A - Integration by parts and boundary conditions

The Equation (4), which is reported here for the sake of readability, has to be integrated by part:

$$\int_{t_1}^{t_2}\Big(\int_0^{\gamma_1 L}\rho A\frac{\partial v_1(z,t)}{\partial t}\delta\frac{\partial v_1(z,t)}{\partial t}\,\mathrm{dz}+\int_{\gamma_1 L}^{\gamma_2 L}\rho A\frac{\partial v_2(z,t)}{\partial t}\delta\frac{\partial v_2(z,t)}{\partial t}\,\mathrm{dz}+$$
$$\int_{\gamma_2 L}^{L}\rho A\frac{\partial v_3(z,t)}{\partial t}\delta\frac{\partial v_3(z,t)}{\partial t}\,\mathrm{dz}+\frac{1}{2}\int_{\gamma_1 L}^{\gamma_2 L}M\frac{\partial v_2(z,t)}{\partial t}\delta\frac{\partial v_2(z,t)}{\partial t}\,\mathrm{dz}-$$
$$\int_0^{\gamma_1 L}\left(EI\frac{\partial^2 v_1(z,t)}{\partial z^2}\delta\frac{\partial^2 v_1(z,t)}{\partial z^2}-(e_0a)^2\rho A\frac{\partial^2 v_1(z,t)}{\partial t^2}\delta\frac{\partial^2 v_1(z,t)}{\partial z^2}\right)\mathrm{dz}-$$
$$\int_{\gamma_1 L}^{\gamma_2 L}\left(EI\frac{\partial^2 v_2(z,t)}{\partial z^2}\delta\frac{\partial^2 v_2(z,t)}{\partial z^2}-(e_0a)^2\rho A\frac{\partial^2 v_2(z,t)}{\partial t^2}\delta\frac{\partial^2 v_2(z,t)}{\partial z^2}\right)\mathrm{dz}-$$
$$\int_{\gamma_2 L}^{L}\left(EI\frac{\partial^2 v_3(z,t)}{\partial z^2}\delta\frac{\partial^2 v_3(z,t)}{\partial z^2}-(e_0a)^2\rho A\frac{\partial^2 v_3(z,t)}{\partial t^2}\delta\frac{\partial^2 v_3(z,t)}{\partial z^2}\right)\mathrm{dz}\Big)\mathrm{dt}=0. \tag{A1}$$

The integrations by parts have been performed as follows:

$$\int_0^{\gamma_1 L}\int_{t_1}^{t_2}\rho A\frac{\partial v_1(z,t)}{\partial t}\delta\frac{\partial v_1(z,t)}{\partial t}\,\mathrm{dt}=\int_0^{\gamma_1 L}\left[\rho A\frac{\partial v_1(z,t)}{\partial t}\delta v_1(z,t)\right]_{t_1}^{t_2}\mathrm{dz}-$$
$$\int_0^{\gamma_1 L}\int_{t_1}^{t_2}\rho A\frac{\partial^2 v_1(z,t)}{\partial t^2}\delta v_1(z,t)\,\mathrm{dt}\,\mathrm{dz};$$
$$\int_{\gamma_1 L}^{\gamma_2 L}\int_{t_1}^{t_2}\rho A\frac{\partial v_2(z,t)}{\partial t}\delta\frac{\partial v_2(z,t)}{\partial t}\,\mathrm{dt}=\int_{\gamma_1 L}^{\gamma_2 L}\left[\rho A\frac{\partial v_2(z,t)}{\partial t}\delta \mathrm{v}_2(z,t)\right]_{t_1}^{t_2}\mathrm{dz}-$$
$$\int_{\gamma_1 L}^{\gamma_2 L}\int_{t_1}^{t_2}\rho A\frac{\partial^2 v_2(z,t)}{\partial t^2}\delta v_2(z,t)\,\mathrm{dt}\,\mathrm{dz};$$
$$\int_{\gamma_2 L}^{L}\int_{t_1}^{t_2}\rho A\frac{\partial v_3(z,t)}{\partial t}\delta\frac{\partial v_3(z,t)}{\partial t}\,\mathrm{dt}\,\mathrm{dz}=\int_{\gamma_2 L}^{L}\left[\rho A\frac{\partial v_3(z,t)}{\partial t}\delta v_3(z,t)\right]_{t_1}^{t_2}\mathrm{dz}-$$
$$\int_{\gamma_2 L}^{L}\int_{t_1}^{t_2}\rho A\frac{\partial^2 v_3(z,t)}{\partial t^2}\delta v_3(z,t)\,\mathrm{dt}\,\mathrm{dz};$$
$$\int_{\gamma_1 L}^{\gamma_2 L}\int_{t_1}^{t_2}M\frac{\partial v_2(z,t)}{\partial t}\delta\frac{\partial v_2(z,t)}{\partial t}\,\mathrm{dt}\,\mathrm{dz}=\int_{\gamma_1 L}^{\gamma_2 L}\left[M\frac{\partial v_2(z,t)}{\partial t}\delta v_2(z,t)\right]_{t_1}^{t_2}\mathrm{dz}-$$
$$\int_{\gamma_1 L}^{\gamma_2 L}\int_{t_1}^{t_2}M\frac{\partial^2 v_2(z,t)}{\partial t^2}\delta v_2(z,t)\,\mathrm{dt}\,\mathrm{dz}; \tag{A2}$$

$$\int_{t_1}^{t_2}\int_0^{\gamma_1 L}(e_0a)^2\,\rho A\frac{\partial^2 v_1(z,t)}{\partial t^2}\delta\frac{\partial^2 v_1(z,t)}{\partial z^2}\,\mathrm{dz}\,\mathrm{dt}=$$
$$\int_{t_1}^{t_2}\left[(e_0a)^2\,\rho A\frac{\partial^2 v_1(z,t)}{\partial t^2}\delta\frac{\partial v_1(z,t)}{\partial z}\right]_0^{\gamma_1 L}\mathrm{dt}-\int_{t_1}^{t_2}\left[(e_0a)^2\,\rho A\frac{\partial^3 v_1(z,t)}{\partial t^2\partial z}\delta v_1(z,t)\right]_0^{\gamma_1 L}\mathrm{dt}+$$
$$\int_{t_1}^{t_2}\int_0^{\gamma_1 L}(e_0a)^2\,\rho A\frac{\partial^4 v_1(z,t)}{\partial t^2\partial z^2}\delta v_1(z,t)\,\mathrm{dz}\,\mathrm{dt}; \tag{A3}$$

$$\int_{t_1}^{t_2}\int_{\gamma_1 L}^{\gamma_2 L}(e_0a)^2\,\rho A\frac{\partial^2 v_2(z,t)}{\partial t^2}\delta\frac{\partial^2 v_2(z,t)}{\partial z^2}\,\mathrm{dz}\,\mathrm{dt}=$$
$$\int_{t_1}^{t_2}\left[(e_0a)^2\,\rho A\frac{\partial^2 v_2(z,t)}{\partial t^2}\delta\frac{\partial v_2(z,t)}{\partial z}\right]_{\gamma_1 L}^{\gamma_2 L}\mathrm{dt}-\int_{t_1}^{t_2}\left[(e_0a)^2\,\rho A\frac{\partial^3 v_2(z,t)}{\partial t^2\partial z}\delta v_2(z,t)\right]_{\gamma_1 L}^{\gamma_2 L}\mathrm{dt}+$$
$$\int_{t_1}^{t_2}\int_{\gamma_1 L}^{\gamma_2 L}(e_0a)^2\,\rho A\frac{\partial^4 v_2(z,t)}{\partial t^2\partial z^2}\delta v_2(z,t)\,\mathrm{dz}\,\mathrm{dt}; \tag{A4}$$

$$\int_{t_1}^{t_2}\int_{\gamma_2 L}^{L}(e_0a)^2\,\rho A\frac{\partial^2 v_3(z,t)}{\partial t^2}\delta\frac{\partial^2 v_3(z,t)}{\partial z^2}\,\mathrm{dz}\,\mathrm{dt}=$$
$$\int_{t_1}^{t_2}\left[(e_0a)^2\,\rho A\frac{\partial^2 v_3(z,t)}{\partial t^2}\delta\frac{\partial v_3(z,t)}{\partial z}\right]_{\gamma_2 L}^{L}\mathrm{dt}-\int_{t_1}^{t_2}\left[(e_0a)^2\,\rho A\frac{\partial^3 v_3(z,t)}{\partial t^2\partial z}\delta v_3(z,t)\right]_{\gamma_2 L}^{L}\mathrm{dt}+$$
$$\int_{t_1}^{t_2}\int_{\gamma_2 L}^{L}(e_0a)^2\,\rho A\frac{\partial^4 v_3(z,t)}{\partial t^2\partial z^2}\delta v_3(z,t)\,\mathrm{dz}\,\mathrm{dt};\tag{A5}$$

and:

$$-\int_{t_1}^{t_2}\int_{0}^{\gamma_1 L}\mathrm{EI}\,\frac{\partial^2 v_1(z,t)}{\partial z^2}\delta\frac{\partial^2 v_1(z,t)}{\partial z^2}\,\mathrm{dz}\,\mathrm{dt}=-\int_{t_1}^{t_2}\left[\mathrm{EI}\,\frac{\partial^2 v_1(z,t)}{\partial z^2}\delta\frac{\partial v_1(z,t)}{\partial z}\right]_{0}^{\gamma_1 L}\mathrm{dt}+$$
$$\int_{t_1}^{t_2}\left[\mathrm{EI}\,\frac{\partial^3 v_1(z,t)}{\partial z^3}\delta v_1(z,t)\right]_{0}^{\gamma_1 L}\mathrm{dt}-\int_{t_1}^{t_2}\int_{0}^{\gamma_1 L}\mathrm{EI}\,\frac{\partial^4 v_1(z,t)}{\partial z^4}\delta v_1(z,t)\,\mathrm{dz}\,\mathrm{dt};\tag{A6}$$

$$-\int_{t_1}^{t_2}\int_{\gamma_1 L}^{\gamma_2 L}\mathrm{EI}\,\frac{\partial^2 v_2(z,t)}{\partial z^2}\delta\frac{\partial^2 v_2(z,t)}{\partial z^2}\,\mathrm{dz}\,\mathrm{dt}=-\int_{t_1}^{t_2}\left[\mathrm{EI}\,\frac{\partial^2 v_2(z,t)}{\partial z^2}\delta\frac{\partial v_2(z,t)}{\partial z}\right]_{\gamma_1 L}^{\gamma_2 L}\mathrm{dt}+$$
$$\int_{t_1}^{t_2}\left[\mathrm{EI}\,\frac{\partial^3 v_2(z,t)}{\partial z^3}\delta v_2(z,t)\right]_{\gamma_1 L}^{\gamma_2 L}\mathrm{dt}-\int_{t_1}^{t_2}\int_{\gamma_1 L}^{\gamma_2 L}\mathrm{EI}\,\frac{\partial^4 v_2(z,t)}{\partial z^4}\delta v_2(z,t)\,\mathrm{dz}\,\mathrm{dt},\tag{A7}$$

$$-\int_{t_1}^{t_2}\int_{\gamma_2 L}^{L}\mathrm{EI}\,\frac{\partial^2 v_3(z,t)}{\partial z^2}\delta\frac{\partial^2 v_3(z,t)}{\partial z^2}\,\mathrm{dz}\,\mathrm{dt}=-\int_{t_1}^{t_2}\left[EI\frac{\partial^2 v_3(z,t)}{\partial z^2}\delta\frac{\partial v_3(z,t)}{\partial z}\right]_{\gamma_2 L}^{L}\mathrm{dt}+$$
$$\int_{t_1}^{t_2}\left[\mathrm{EI}\,\frac{\partial^3 v_3(z,t)}{\partial z^3}\delta v_3(z,t)\right]_{0}^{L}\mathrm{dt}-\int_{t_1}^{t_2}\int_{\gamma_2 L}^{L}\mathrm{EI}\,\frac{\partial^4 v_3(z,t)}{\partial z^4}\delta v_3(z,t)\,\mathrm{dz}\,\mathrm{dt}\,.\tag{A8}$$

Finally, the following system of three equations of motion has been obtained:

$$\mathrm{EI}\,\frac{\partial^4 v_1(z,t)}{\partial z^4} - (e_0 a)^2\,\rho A\frac{\partial^4 v_1(z,t)}{\partial z^2\partial t^2} + \rho A\frac{\partial^2 v_1(z,t)}{\partial t^2} = 0,\ 0 < z < \gamma_1 L$$
$$\mathrm{EI}\,\frac{\partial^4 v_2(z,t)}{\partial z^4} - (e_0 a)^2\,\rho A\frac{\partial^4 v_2(z,t)}{\partial z^2\partial t^2} + (\rho A + M)\frac{\partial^2 v_2(z,t)}{\partial t^2} = 0, \gamma_1 L < z < \gamma_2 L$$
$$\mathrm{EI}\,\frac{\partial^4 v_3(z,t)}{\partial z^4} - (e_0 a)^2\,\rho A\frac{\partial^4 v_3(z,t)}{\partial z^2\partial t^2} + \rho A\frac{\partial^2 v_3(z,t)}{\partial t^2} = 0, \gamma_2 L < z < L; \quad \text{(A9)}$$

together with the following particular boundary conditions:

$$v_1(0,t) = 0, \tag{A10}$$

$$\frac{\partial v_1(0,t)}{\partial z} = 0, \tag{A11}$$

for $z = 0$ and for $z = L$:

$$\mathrm{EI}\,\frac{\partial^3 v_3(L,t)}{\partial z^3} - (e_0 a)^2\,\rho A\frac{\partial^3 v_3(L,t)}{\partial t^2\partial z} = 0, \tag{A12}$$

$$-\mathrm{EI}\,\frac{\partial^2 v_3(L,t)}{\partial z^2} + (e_0 a)^2\,\rho A\frac{\partial^2 v_3(L,t)}{\partial t^2} = 0. \tag{A13}$$

The boundary conditions for $z = \gamma_1 L$ are:

$$\begin{gathered}
v_1(\gamma_1 L,t) = v_2(\gamma_1 L,t)\\
\frac{\partial v_1(\gamma_1 L,t)}{\partial z} = \frac{\partial v_2(\gamma_1 L,t)}{\partial z}\\
(e_0 a)^2\,\rho A\frac{\partial^3 v_1(\gamma_1 L,t)}{\partial t^2\partial z} - \mathrm{EI}\,\frac{\partial^3 v_1(\gamma_1 L,t)}{\partial z^3} - (e_0 a)^2\,\rho A\frac{\partial^3 v_2(\gamma_1 L,t)}{\partial t^2\partial z} + \mathrm{EI}\,\frac{\partial^3 v_2(\gamma_1 L,t)}{\partial z^3} = 0\\
(e_0 a)^2\,\rho A\frac{\partial^2 v_1(\gamma_1 L,t)}{\partial t^2} - EI\frac{\partial^2 v_1(\gamma_1 L,t)}{\partial z^2} - (e_0 a)^2\,\rho A\frac{\partial^2 v_2(\gamma_1 L,t)}{\partial t^2} + \mathrm{EI}\,\frac{\partial^2 v_2(\gamma_1 L,t)}{\partial z^2} = 0,
\end{gathered} \tag{A14}$$

and at $z = \gamma_2 L$:

$$
\begin{aligned}
v_2\left(\gamma_2 L,t\right) &= v_3\left(\gamma_2 L,t\right)\\
\frac{\partial v_2\left(\gamma_2 L,t\right)}{\partial z} &= \frac{\partial v_3\left(\gamma_2 L,t\right)}{\partial z}\\
\left(e_0 a\right)^2 \rho A\frac{\partial^3 v_2\left(\gamma_2 L,t\right)}{\partial t^2 \partial z} - \mathrm{EI}\,\frac{\partial^3 v_2\left(\gamma_2 L,t\right)}{\partial z^3} - \left(e_0 a\right)^2 \rho A\frac{\partial^3 v_3\left(\gamma_2 L,t\right)}{\partial t^2 \partial z} + EI\frac{\partial^3 v_3\left(\gamma_2 L,t\right)}{\partial z^3} &= 0\\
+\left(e_0 a\right)^2 \rho A\frac{\partial^2 v_2\left(\gamma_2 L,t\right)}{\partial t^2} - EI\frac{\partial^2 v_2\left(\gamma_2 L,t\right)}{\partial z^2} - \left(e_0 a\right)^2 \rho A\frac{\partial^2 v_3\left(\gamma_2 L,t\right)}{\partial t^2} + EI\frac{\partial^2 v_3\left(\gamma_2 L,t\right)}{\partial z^2} &= 0.
\end{aligned}
\tag{A15}
$$

Appendix B - Integration by parts

The Equation (10), which is reported here for the sake of readability, has to be integrated by part:

$$
\begin{aligned}
&\int_0^L \mathrm{EI}\,\frac{\partial^4 v(z)}{\partial z^4} y(z)\mathrm{dz} + \omega^2 \int_0^L \left(e_0 a\right)^2 \rho\mathrm{A}\frac{\partial^2 v(z)}{\partial z^2} y(z)\mathrm{dz} -\\
&\omega^2 \int_0^L \rho\mathrm{A} v(z) y(z)\mathrm{dz} - \omega^2 \int_{\gamma_1 L}^{\gamma_2 L} \mathrm{m} v(z) y(z)\mathrm{dz} = 0.
\end{aligned}
\tag{B1}
$$

where $v(z)$ denotes the displacement function along the whole span. Two successive integrations by parts can be performed:

$$
\begin{aligned}
&\int_0^L \mathrm{EI}\,\frac{\partial^4 v(z)}{\partial z^4} y(z)\mathrm{dz} = \left[\mathrm{EI}\,\frac{\partial^3 v(z)}{\partial z^3} y(z)\right]_0^L - \int_0^L \mathrm{EI}\frac{\partial^3 v(z)}{\partial z^3}\frac{\partial y(z)}{\partial z}\mathrm{dz} =\\
&\left[\mathrm{EI}\,\frac{\partial^3 v(z)}{\partial z^3} y(z)\right]_0^L - \left[\mathrm{EI}\,\frac{\partial^2 v(z)}{\partial z^2}\frac{\partial y(z)}{\partial z}\right]_0^L + \int_0^L \mathrm{EI}\,\frac{\partial^2 v(z)}{\partial z^2}\frac{\partial^2 y(z)}{\partial z^2}\mathrm{dz},
\end{aligned}
\tag{B2}
$$

and one gets:

$$\omega^2 \int_0^L (e_0 a)^2 \rho \mathrm{A} \frac{\partial^2 v(z)}{\partial z^2} y(z) \mathrm{dz} =$$
$$\left[\omega^2 (e_0 a)^2 \rho \mathrm{A} \frac{\partial v(z)}{\partial z} y(z)\right]_0^L - \int_0^L \omega^2 (e_0 a)^2 \rho \mathrm{A} \frac{\partial v(z)}{\partial z} \frac{\partial y(z)}{\partial z} \mathrm{dz} =$$
$$\left[\omega^2 (e_0 a)^2 \rho \mathrm{A} \frac{\partial v(z)}{\partial z} y(z)\right]_0^L - \left[\omega^2 (e_0 a)^2 \rho \mathrm{A} v(z) \frac{\partial y(z)}{\partial z}\right]_0^L +$$
$$\int_0^L \omega^2 (e_0 a)^2 \rho \mathrm{A} v(z) \frac{\partial^2 y(z)}{\partial z^2} \mathrm{dz}. \tag{B3}$$

Finally, the Equation (10) becomes:

$$\int_0^L \mathrm{EI} \frac{\partial^2 v(z)}{\partial z^2} \frac{\partial^2 y(z)}{\partial z^2} \mathrm{dz} - \omega^2 \int_0^L \rho \mathrm{A} v(z) y(z) \mathrm{dz} - \omega^2 \int_{\gamma_1 L}^{\gamma_2 L} \mathrm{m} v(z) y(z) \mathrm{dz} +$$
$$\int_0^L \omega^2 (e_0 a)^2 \rho \mathrm{A} v(z) \frac{\partial^2 y(z)}{\partial z^2} \mathrm{dz} + \left[\mathrm{EI} \frac{\partial^3 v(z)}{\partial z^3} y(z)\right]_0^L - \left[\mathrm{EI} \frac{\partial^2 v(z)}{\partial z^2} \frac{\partial y(z)}{\partial z}\right]_0^L +$$
$$\left[\omega^2 (e_0 a)^2 \rho \mathrm{A} \frac{\partial v(z)}{\partial z} y(z)\right]_0^L - \left[\omega^2 (e_0 a)^2 \rho \mathrm{A} v(z) \frac{\partial y(z)}{\partial z}\right]_0^L = 0. \tag{B4}$$

Figure1

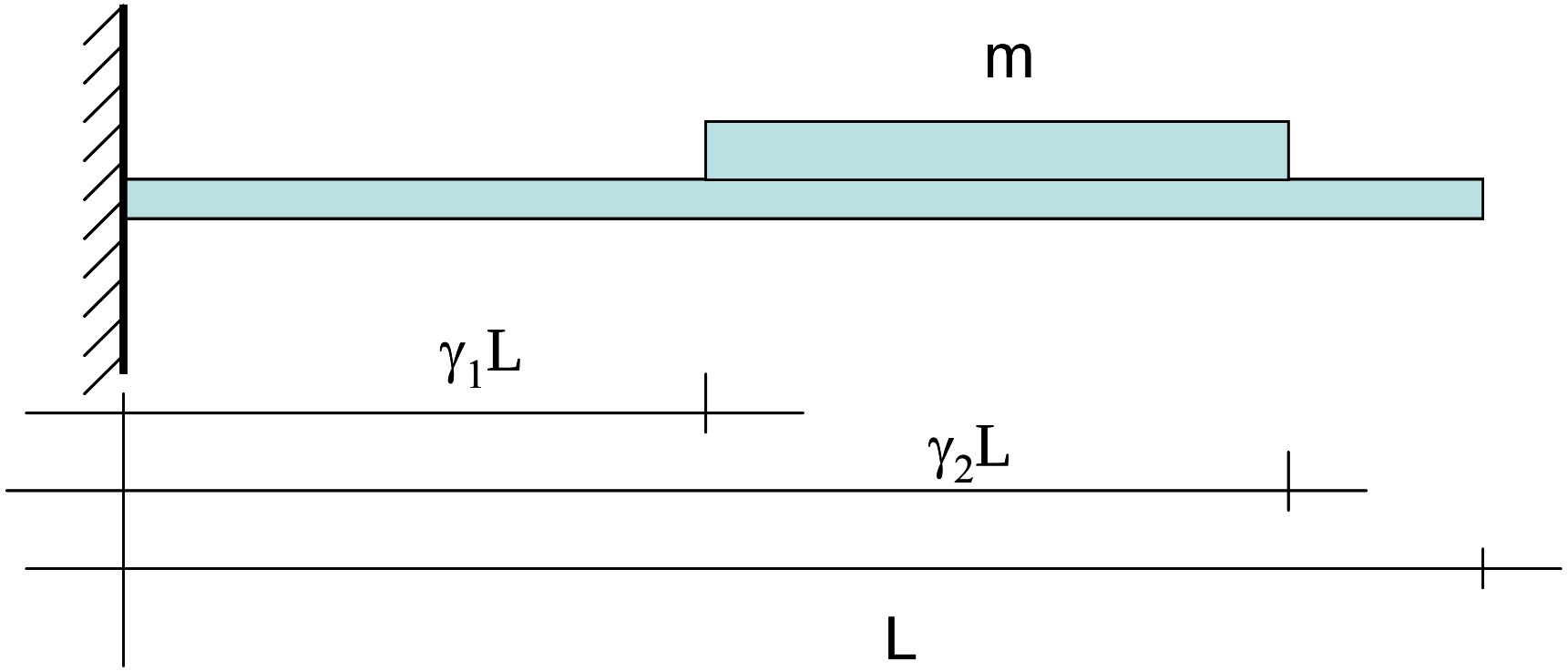

Figure2

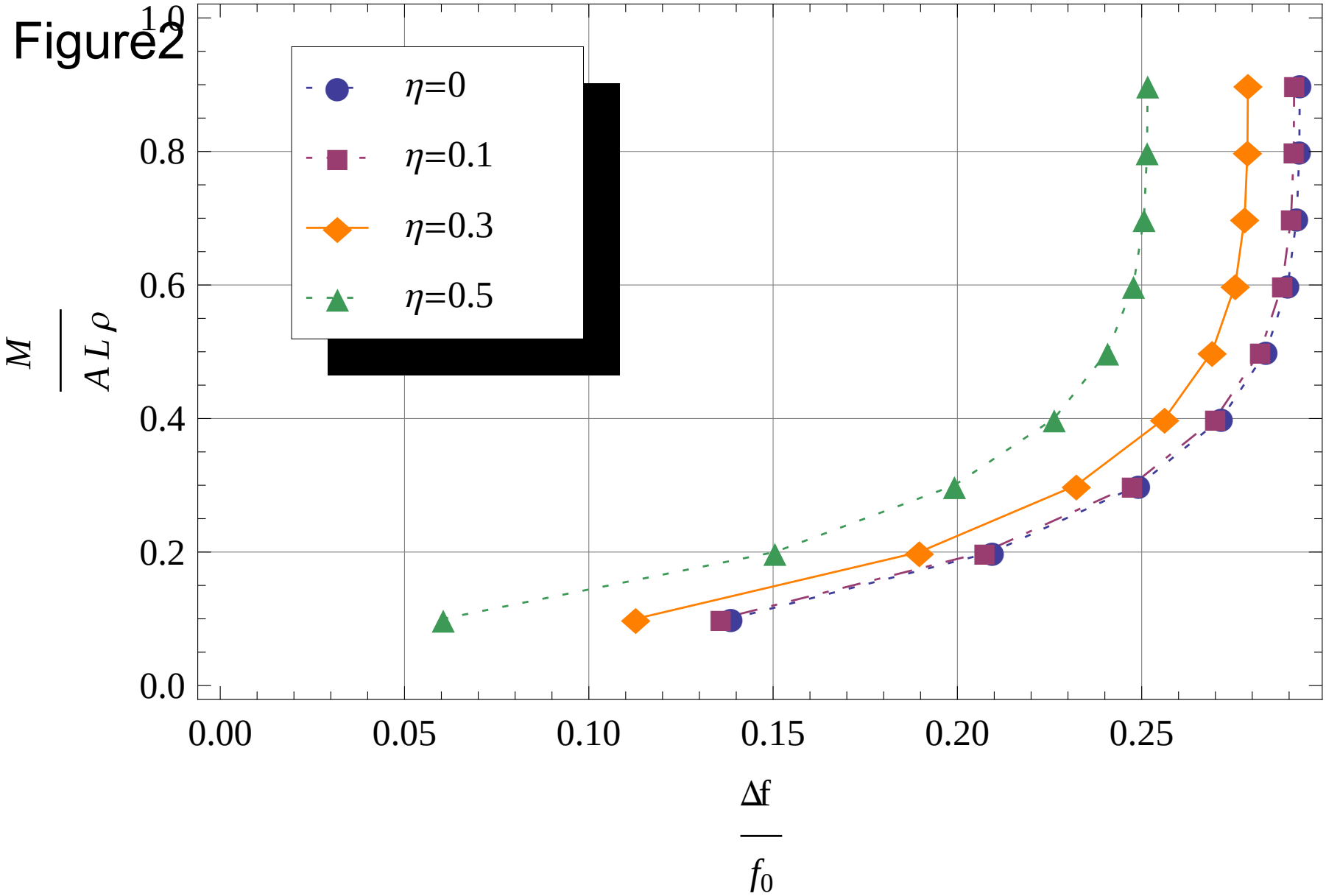

Figure3

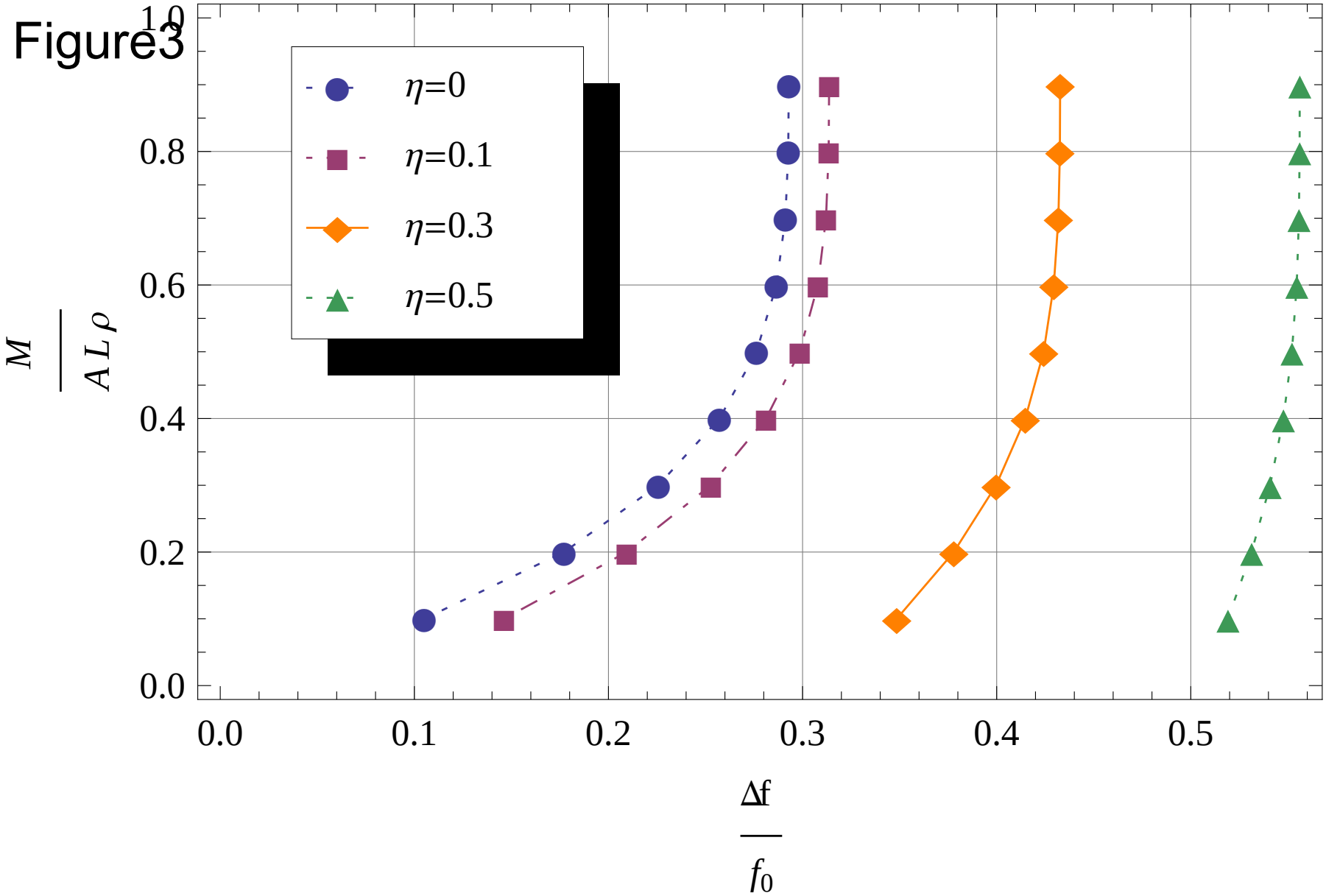

Figure4

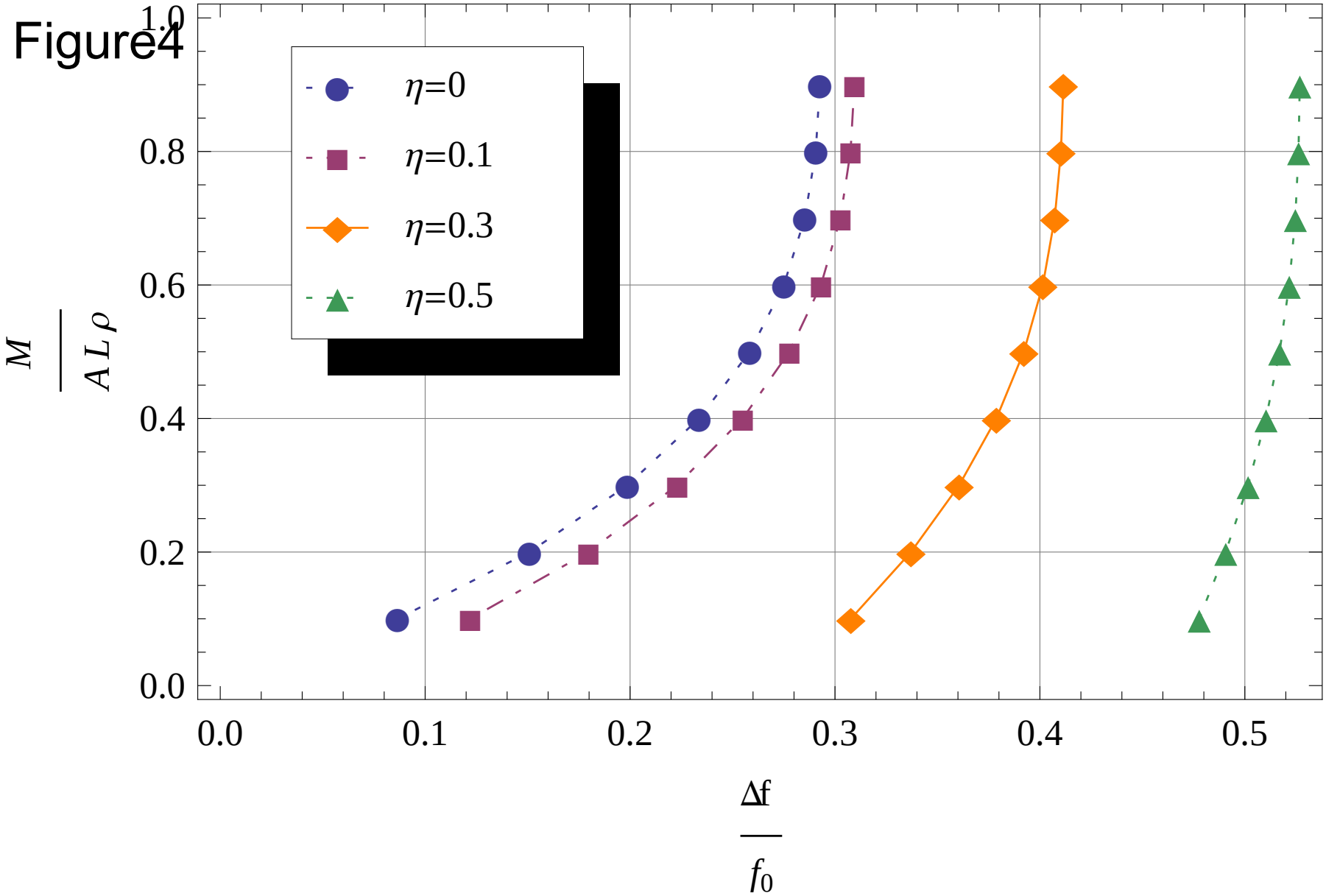

Figure5

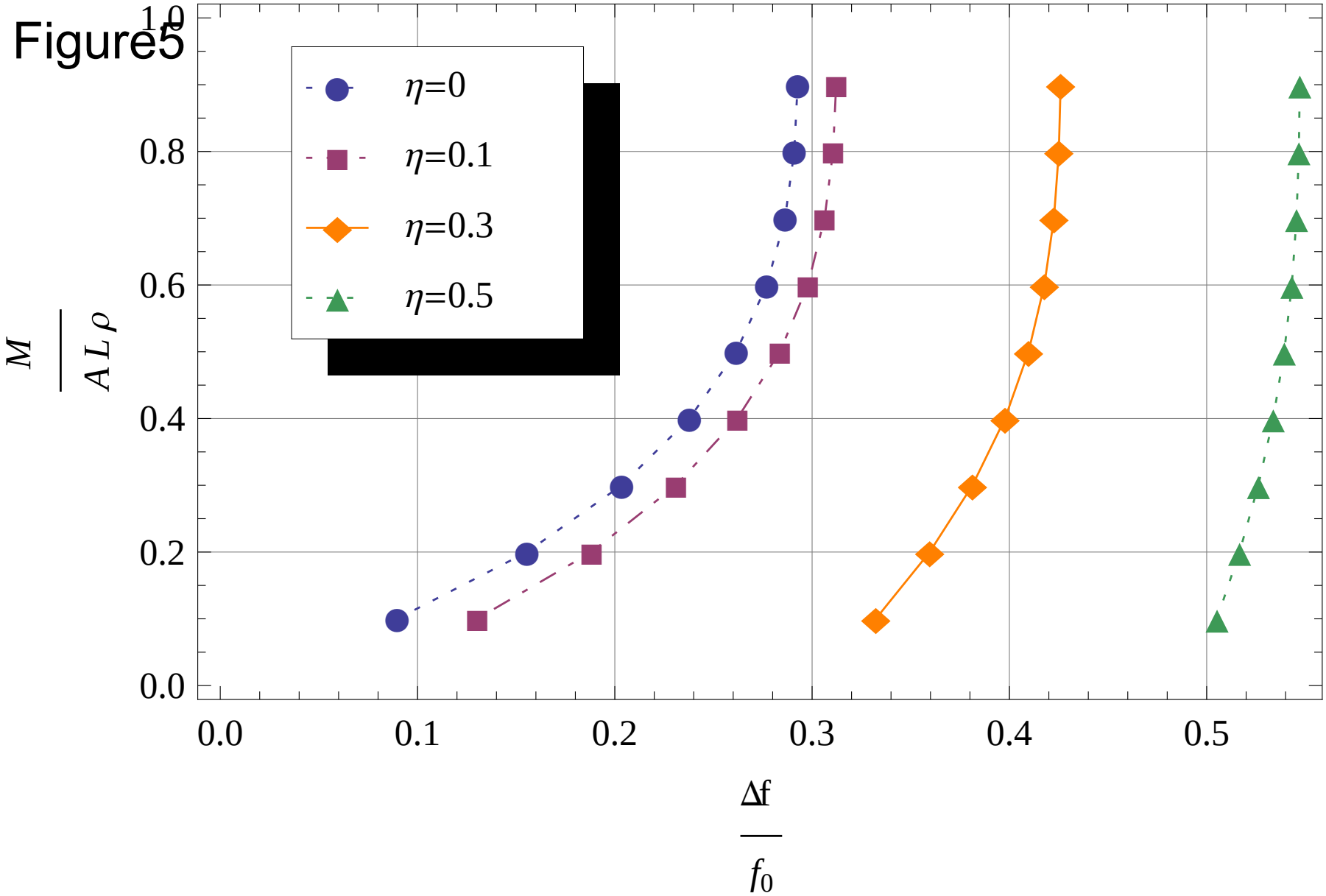

Figure6